CANADIAN JOURNAL OF RESEARCH

VOLUME 28 DECEMBER, 1950 NUMBER 12

— SECTION B —

CHEMICAL SCIENCES

Contents

Page

Use of Liquid Ammonia in the Fractionation of Wheat Straw Holocellulose—*C. T. Bishop and G. A. Adams* - - - 753

The New Complex Compounds of Arginine and Lysine—*Alfred Taurins* - - - - - - - - - - - - - 762

Flocculation in Suspensions of Large Particles—*C. E. Hubley, A. A. Robertson, and S. G. Mason* - - - - - - - 770

Volumetric Determination of Small Amounts of Iridium—*W. A. E. McBryde and M. L. Cluett* - - - - - - - 788

The Oxidation of Carbon Monoxide by Solid Silver Permanganate Reagents. II. Kinetic Studies with Silver Permanganate-Zinc Oxide—*Morris Katz, G. A. Grant, and R. Riberdy* - - - - - - - - - - - - - - - 799

NATIONAL RESEARCH COUNCIL
OTTAWA, CANADA

CANADIAN JOURNAL OF RESEARCH

The *Canadian Journal of Research* is issued in six sections, as follows:

A. Physical Sciences	D. Zoological Sciences
B. Chemical Sciences	E. Medical Sciences
C. Botanical Sciences	F. Technology

For the present, Sections A, C, D, and E are to be issued six times annually, and Sections B and F, twelve times annually, each under separate cover, with separate pagination.

The *Canadian Journal of Research* is published by the National Research Council of Canada under authority of the Chairman of the Committee of the Privy Council on Scientific and Industrial Research. The *Canadian Journal of Research* is edited by a joint Editorial Board consisting of members of the National Research Council of Canada, the Royal Society of Canada, and the Chemical Institute of Canada.

Sections B and F of the *Canadian Journal of Research* have been chosen by the Chemical Institute of Canada as its medium of publication for scientific papers.

EDITORIAL BOARD

Representing
NATIONAL RESEARCH COUNCIL

DR. H. P. ARMES (*Chairman*),
Dean of the University,
University of Manitoba,
Winnipeg, Man.

DR. OTTO MAASS,
Macdonald Professor of Physical Chemistry,
McGill University,
Montreal, P.Q.

DR. J. H. L. JOHNSTONE,
Professor of Physics,
Dalhousie University,
Halifax, N.S.

DR. A. BERTRAND,
Professor of Bacteriology,
Faculty of Medicine,
University of Montreal,
Montreal, P.Q.

Representing
ROYAL SOCIETY OF CANADA

DR. G. M. VOLKOFF,
Professor of Physics,
University of British Columbia,
Vancouver, B.C.

DR. J. W. T. SPINKS,
Dean, College of Graduate Studies,
University of Saskatchewan,
Saskatoon.

Section III

DR. H. S. JACKSON,
Head, Department of Botany,
University of Toronto,
Toronto.

DR. E. HORNE CRAIGIE,
Department of Zoology,
University of Toronto,
Toronto.

Section V

Ex officio

DR. LÉO MARION, Editor-in-Chief,
Division of Chemistry,
National Research Laboratories,
Ottawa.

DR. H. H. SAUNDERSON,
Director, Division of Information Services,
National Research Council,
Ottawa.

Representing
THE CHEMICAL INSTITUTE OF CANADA

DR. H. G. THODE,
Department of Chemistry,
McMaster University,
Hamilton.

EDITORIAL COMMITTEE

Editor-in-Chief,	DR. LÉO MARION	Editor, Section D,	DR. E. HORNE CRAIGIE
Editor, Section A,	DR. G. M. VOLKOFF	Editor, Section E,	DR. J. B. COLLIP
Editor, Section B,	DR. J. W. T. SPINKS DR. H. G. THODE	Editor, Section F,	DR. J. A. ANDERSON DR. G. M. VOLKOFF DR. H. G. THODE
Editor, Section C,	DR. H. S. JACKSON		

Manuscripts should be addressed:

Editor-in-Chief,
Canadian Journal of Research,
National Research Council, Ottawa, Canada.

NOTICE

The Canadian Journal of Research is at present published in six sections, A to F. Starting with January 1, 1951, these sections will be published as separate journals under distinctive names and the designation Canadian Journal of Research will no longer be used. The present names and the corresponding new names are as follows:

Present Name	*New Name*
Canadian Journal of Research, Section A (Physical Sciences)	Canadian Journal of Physics
Canadian Journal of Research, Section B (Chemical Sciences)	Canadian Journal of Chemistry
Canadian Journal of Research, Section C (Botanical Sciences)	Canadian Journal of Botany
Canadian Journal of Research, Section D (Zoological Sciences)	Canadian Journal of Zoology
Canadian Journal of Research, Section E (Medical Sciences)	Canadian Journal of Medical Sciences
Canadian Journal of Research, Section F (Technological Sciences)	Canadian Journal of Technology

In order to preserve continuity the present sequence of volume numbers will be retained, and in each case the volume for 1951 will be Volume 29.

The subscription rates for the Journals will remain as at present.

Canadian Journal of Research

Issued by THE NATIONAL RESEARCH COUNCIL OF CANADA

VOL. 28, SEC. B. DECEMBER, 1950 NUMBER 12

USE OF LIQUID AMMONIA IN THE FRACTIONATION OF WHEAT STRAW HOLOCELLULOSE[1]

BY C. T. BISHOP AND G. A. ADAMS

Abstract

Wheat straw holocellulose, after soaking in liquid ammonia for 36 hr. at room temperature, was fractionated by successive extractions with cold water, 0.5% sodium carbonate, 0.5% potassium hydroxide, and 2.2% potassium hydroxide. Pretreatment with liquid ammonia increased the material soluble in cold water from 3% to 20.2%. Hemicellulose fractions were precipitated from the extracts by ethanol. A complete analytical balance was obtained by estimating ash, pentosan, uronic acid anhydride, acetyl, and methoxyl contents of the original holocellulose, of each of the fractions and of the residue. Analyses of the isolated fractions showed some systematic differences, with pentosan contents increasing and uronic acid anhydride decreasing progressively in the alkali soluble fractions. D-xylose, L-arabinose, D-glucose, D-galactose, and hexuronic acid in approximate molar ratios of 40: 7: 2: 1: 4 were found in the hemicellulose fractions. The presence of the sugars was confirmed by isolation of crystalline derivatives. A uronic acid complex, resistant to hydrolysis, was isolated and the components shown to be D-xylose and a monomethoxyl galacturonic acid.

Introduction

The fractionation of holocelluloses has always been empirical and no procedures have been accepted as standard. One method, described by O'Dwyer (26), consisted of extracting holocellulose with alkali and precipitating hemicellulose fractions by the successive addition of acid and ethanol to the extract. This procedure has been used extensively in studying hemicelluloses for the last 20 years (25, 27, 28, 29, 36). Preece (31) showed that alkali degraded the hemicelluloses and in recent years attempts have been made to isolate hemicellulose fractions in their native state by using milder, neutral solvents. Mitchell and Ritter (20) extracted hemicelluloses from maple wood holocellulose with water followed by extractions with increasingly stronger alkaline solutions. A similar method was used by Millett and Stamm (19) in fractionating aspen holocellulose.

Anhydrous liquid ammonia is generally regarded as a neutral solvent (7) and has been used extensively as a solvent for carbohydrate reactions (8, 18, 21, 22). Yan (37) reported that liquid ammonia extracted 0.8% of polysaccharide material from maple wood, and removed (as acetamide) the entire acetyl content of the wood. Neubauer (23) found that hot water could extract about 2% of polysaccharide material, not previously water soluble, from the

[1] *Manuscript received August 22, 1950.*
Contribution from the Division of Applied Biology, National Research Laboratories, Ottawa. Issued as Paper No. 96 on the Industrial Utilization of Wastes and Surpluses, and as N.R.C. No. 2252.

ammonia extracted wood residue. Though deacetylation was caused by liquid ammonia, a physical interpretation of its action was favored, i.e., swelling of the fiber structure of the wood by liquid ammonia increased the accessibility of the polysaccharides. Hess and Gundermann (11) showed, by X-ray diffraction patterns, that pure cellulose fibers were swollen by liquid ammonia.

Buston (3) examined hemicelluloses extracted by alkali from several forage grasses and found large amounts of D-xylose and L-arabinose. Extraction of oat hulls with 5% sodium hydroxide removed a mixture of hemicelluloses in which Anderson and Krznarich (2) identified D-xylose, L-arabinose, D-galactose, and D-glucuronic acid. The presence of xylan in wheat straw was established as early as 1892 (32) and commercial production of D-xylose from this agricultural waste product has been investigated (6, 17). Norris and Preece (25) found D-xylose, L-arabinose, and an unidentified uronic acid in hemicelluloses isolated from wheat bran according to the method of O'Dwyer (26). D-xylose, L-arabinose, and a uronic acid in molar ratios of 23: 0.9: 1 were found in hemicellulose fractions of wheat straw by Weihe and Phillips (36).

Although the present knowledge of hemicelluloses from woods is quite extensive much less is known about the corresponding materials from grasses and straws. The purpose of the present work was to fractionate wheat straw holocellulose after pretreatment with anhydrous liquid ammonia, study the fractionation in detail by analysis, and establish the identities and relative amounts of the constituent sugars of the hemicellulose fractions.

Materials and Methods

Wheat straw holocellulose was prepared from extractive-free wheat straw by a delignification procedure using sodium chlorite, as previously described by Adams and Castagne (1). Pentoses were determined as furfural, by the excess bromine oxidation method of Hughes and Acree (13), after distillation from 12% hydrochloric acid. Uronic acid anhydride was determined by the method of Tracy (35); methoxyl by the procedure described by Clarke (5); acetyl content was determined by alkali saponification followed by steam distillation and titration of the acetic acid (5). Reducing sugars were determined by the method of Somogyi (33) and individual sugars, liberated by acid hydrolysis, were determined both qualitatively and quantitatively by a combination of chromatographic techniques (10, 16, 30). Moisture was determined by drying to constant weight at 110°C., ash by incinerating at 600°C., and nitrogen by the Kjeldahl procedure. All analyses were on an ash-free, moisture-free basis unless otherwise noted.

Experimental Procedures and Results

Liquid Ammonia Treatment

In a typical experiment, air dry holocellulose (150 gm.) was placed in a 3 liter flask fitted with a ground glass cap and a side arm with a stopcock. Moisture was removed by continuous pumping under high vacuum (0.1 mm.) for 36 hr. over phosphoric anhydride at room temperature. The flask was

placed in an insulated box and connected through the side arm to a cylinder of liquid ammonia. A slow flow of liquid ammonia was started and sucked into the evacuated flask by slowly opening the stopcock in the side arm. When the pressure inside the flask reached atmospheric the ground glass cap was removed and the flow of liquid ammonia increased. Approximately 1500 ml. of liquid ammonia was used for 150 gm. of holocellulose. The reaction flask was then removed from the insulated box and allowed to stand at room temperature for 36 hr. No mechanical agitation was necessary as the boiling of the ammonia solution provided adequate mixing. Formation of a heavy coating of frost on the outside of the flask greatly retarded ammonia evaporation and permitted the treatment to proceed actively for 24–36 hr. without further attention. At the end of the reaction period the liquid ammonia was pumped off as vapor through anhydrous calcium chloride, by a water aspirator. Last traces, tenaciously held by the holocellulose, were removed at high vacuum (0.1 mm.) over sulphuric acid at room temperature.

Extraction of Hemicellulose Fractions

Preliminary experiments showed that liquid ammonia extracted 10% of the holocellulose. However, because only about 10% of the extracted material was precipitable by alcohol from water solution, it seemed advisable to leave the ammonia extract in the holocellulose and recover it in combination with the aqueous extract. (In a separate investigation the ammonia extract is being recovered by another method and will be reported on later.)

Wheat straw holocellulose that had been treated with liquid ammonia was then successively extracted at room temperature with water, 0.5% sodium carbonate, 0.5% potassium hydroxide, and 2.2% potassium hydroxide. A solid–solvent ratio of approximately 1:8 was used and mixing was provided by a mechanical stirrer. All extractions were exhaustive, as determined by total solids in the extracts, five extractions of 24 hr. each being required. Extractions with water, 0.5% sodium carbonate, 0.5% potassium hydroxide, and 2.2% potassium hydroxide removed 20.2%, 2.12%, 1.84%, and 3.40% of the holocellulose respectively. The total amount of material extracted was 27.6% of the holocellulose.

In the present study the primary role of liquid ammonia was that of a swelling agent making the hemicellulose more accessible to solvents. Water, at room temperature, extracted only 3% of the original holocellulose but after treatment with liquid ammonia 20.2% of the holocellulose was soluble in water. The neutral reaction of liquid ammonia appeared unlikely to cause degradation in the hemicelluloses to the extent of increasing their water solubility. The water extraction was also made under very mild conditions and the pH of 8.0 was much less alkaline than even the 0.5% sodium carbonate extract (pH 10.4).

Isolation of Hemicellulose Fractions

The extracts were adjusted to pH 7.0 with hydrochloric acid and concentrated at about 50°C. in a vacuum evaporator to 1–2% solids. Hemicelluloses

were precipitated by adding three volumes of 95% ethanol and adjusting the pH to 4–5 with dilute hydrochloric acid. The mixtures were allowed to stand overnight at 0°C. to assure complete precipitation. The mother liquors were separately concentrated, and addition of five volumes of 95% ethanol caused a further precipitation only in the aqueous extract. Therefore it was assumed that precipitation of hemicelluloses from the dilute alkali extracts was completed by the first addition of ethanol. The precipitated hemicelluloses were dissolved in water and dialyzed to remove chloride ion completely. The dialyzed materials were reprecipitated, dried through solvent exchange with absolute ethanol and ether and finally to constant weight by high vacuum pumping (0.1 mm.) at room temperature over phosphoric anhydride. The ethanol soluble portions of the extracts were evaporated at room temperature by an air current from an electric fan. These sticky, highly colored residues were dried to constant weight under vacuum over phosphoric anhydride. Fig. 1 is a flow sheet showing

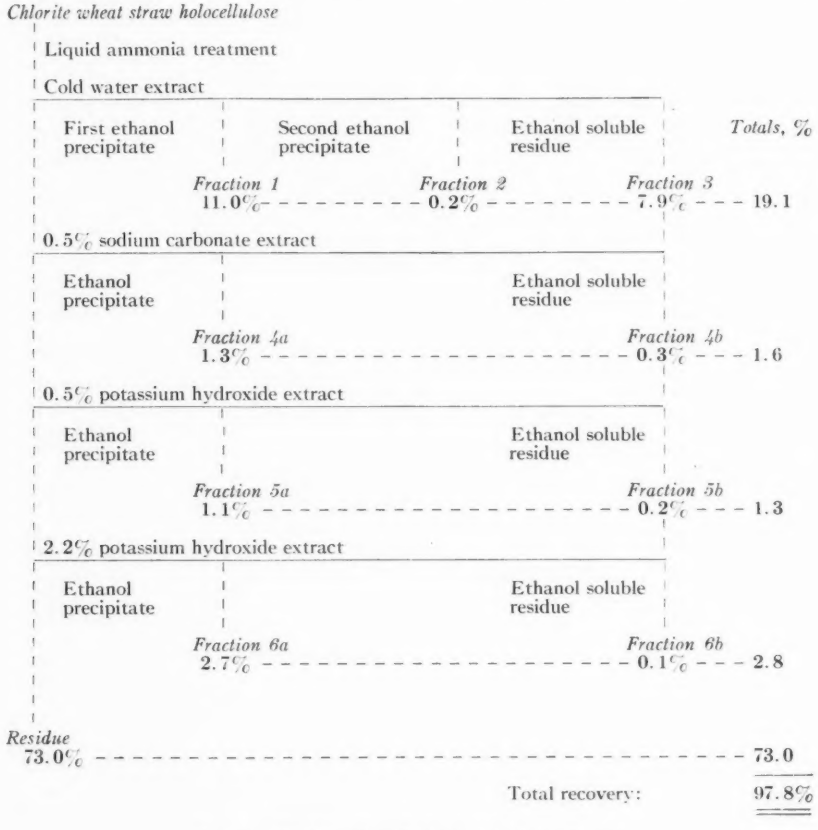

FIG. 1. *Fractionation of wheat straw holocellulose.*

the fractionation of wheat straw holocellulose and the relative amounts of each fraction in terms of per cent of original holocellulose. A total recovery of 97.8% of the original holocellulose after completion of the fractionation was obtained.

Analytical Examination of Fractions

The results of an analytical study of the hemicellulose fractions of wheat straw holocellulose are given in Table I. Although the total material used in the fractionation was almost quantitatively recovered, significant losses of methoxyl, uronic acid anhydride, and pentosan occurred. These losses cannot be explained at the present time. The acetyl content of the original holocellulose was 1.95% of which only 0.09% was recovered, all in Fraction 1. This loss in acetyl content was expected because of the deacetylating action of liquid ammonia shown by Yan (37). Nitrogen contents were generally negligible except in Fraction 3: this was the ethanol soluble residue from the aqueous extracts, and any acetamide, produced from ammonia and acetyl groups, would be found in this fraction.

While analyses of the main fractions (Fractions 1, 2, 4*a*, 5*a* and 6*a*, Table I) showed considerable similarities, certain trends indicate that fractionation had

TABLE I

COMPOSITION (%) OF WHEAT STRAW HOLOCELLULOSE AND EXTRACTED HEMICELLULOSE FRACTIONS
(Averages of duplicate determinations)

Fraction	Description of fraction	Ash	$[\alpha]_D^{20}$	Reducing power*	Nitrogen	Methoxyl	Uronic acid anhydride ($CO_2 \times 4$)	Pentosan**
Holocellulose		2.05			0.2	1.39	5.85	29.5
1	Water extract: First precipitate	0.56	−81.6	0.70	0.3	1.48	7.56	78.5
2	Water extract: Second precipitate	1.36	−72.2	0.58	—	1.89	10.8	74.2
4*a*	0.5% Na_2CO_3 extract: Ethanol precipitate	2.12	−70.5	0.55	—	1.85	9.93	74.9
5*a*	0.5% KOH extract: Ethanol precipitate	0.90	−95.6	0.62	—	1.85	7.69	75.8
6*a*	2.2% KOH extract: Ethanol precipitate	2.05	−87.1	0.18	0.2	0.93	5.48	85.4
3	Water extract: Soluble residue	11.8	—	—	6.2	5.65	6.60	3.1
4*b*	0.5% Na_2CO_3 extract: Soluble residue	34.0	—	—	—	11.6	6.08	11.1
5*b*	0.5% KOH extract: Soluble residue	34.6	—	—	—	12.2	0.0	13.3
6*b*	2.2% KOH extract: Soluble residue	59.1	—	—	—	8.74	0.0	16.4
Residue	Holocellulose after removal of the above fractions	0.98	—	—	0.1	0.16	2.52	10.8

* *Expressed as milliliters of 0.005 N thiosulphate per 10 mgm.*
** *Calculated as xylan corrected for uronic acid anhydride.*

taken place. Uronic acid anhydride contents were high in the first fractions and decreased in the more insoluble fractions. The uronic acids, because of their polar carboxyl groups, are more soluble than pentosans and would therefore tend to be concentrated in the first fractions. Uronic acid anhydride contents of Fractions 3 and 4*b* indicated that some of the polyuronide material was of sufficiently short chain length to escape precipitation by ethanol and was carried through into the soluble residues. Alkali tended to remove pentosan material and except for Fraction 1 the pentosan contents increased in the more insoluble alkali extracts.

Dialysis was successful in reducing the ash contents of the hemicellulose fractions and the greater part of the ash was concentrated in the soluble residues. These soluble residues (Fractions 3, 4*b*, 5*b*, and 6*b*) also had unusually high methoxyl contents. It may be that some of the residual lignin, which made up about 2% of the original holocellulose, was carried over into these fractions. The fractions removed represented the most easily extractable material and the residue still contained a considerable proportion of uronic acid anhydride and pentosan.

Acid Hydrolysis of Hemicellulose Fractions

In a typical experiment the hemicellulose (0.5 gm.) was hydrolyzed by heating with 1% sulphuric acid (50 ml.) on a boiling water bath. The progress of the hydrolysis was followed by changes in reducing power and was stopped when this value reached a maximum; a period of approximately 12 hr. was usually required. The hydrolyses left insoluble residues amounting to 1.4, 7.0, 3.0, 2.9, and 1.6% of Fractions 1, 2, 4*a*, 5*a*, and 6*a*, respectively. These acid insoluble residues strongly resisted further hydrolysis with 5% or 10% sulphuric acid at 120°C. under pressure, and were insoluble in 72% acid under conditions of the Klason lignin determination. It is evident that the residues were noncarbohydrate.

Examination of Constituent Sugars

The acid hydrolyzate of each hemicellulose fraction was neutralized with barium carbonate. The barium salts were removed by filtration, washed with hot water, and the aqueous filtrates and washings concentrated to 50 ml. The constituent sugars were detected by descending paper chromatography as outlined by Partridge (30), with a solvent system of ethyl acetate–pyridine–water as recommended by Jermyn and Isherwood (16) and aniline phthalate as an indicator. Amounts of individual sugars were determined by a method similar to that of Hawthorne (10). The sugars, separated by chromatography, were extracted from the paper, and reducing powers of the extracts were determined. Comparison of these values with reducing powers found for known amounts of the sugar concerned gave a quantitative estimation of each sugar in the hydrolyzates. The results are recorded in Table II. The uniformity in these analyses was unexpected because of the previous trends found in uronic acid anhydride

TABLE II

CONSTITUENT SUGARS (%) OF HEMICELLULOSE FRACTIONS
(Averages of duplicate determinations)

Sugars	Fraction 1	Fraction 2	Fraction 4*a*	Fraction 5*a*	Fraction 6*a*
Xylose	75.0	62.5	65.6	69.0	73.5
Arabinose	9.1	13.3	14.2	12.4	9.2
Glucose	4.2	2.3	3.4	5.2	5.3
Galactose	2.1	2.1	1.9	1.7	2.8

and pentosan contents. On the basis of analyses for individual sugars the hemicellulose fractions all had a similar composition of D-xylose, L-arabinose, D-glucose, D-galactose, and a hexuronic acid in molar ratios of 40: 7: 2: 1: 4.

To confirm the identity of the constituent sugars, 10 gm. of Fraction 1 was hydrolyzed under the conditions previously described. After neutralization, the filtrate from the barium salts was poured into three volumes of 95% ethanol. The barium uronates were precipitated, dried in the usual manner through solvent exchange and desiccation under high vacuum, and examined separately. The alcoholic filtrate was concentrated to a thin syrup from which D-xylose (3.6 gm.) was crystallized. It had a m.p. 145–146°, not depressed on admixture with an authentic sample, and $[\alpha]_D^{20} = +19.9$. In the mother liquors from the xylose crystallization, L-arabinose was identified as the benzoylhydrazone (12), m.p. and mixed m.p. 184–185°; $[\alpha]_D^{20} = +23.8$, found for an authentic sample $[\alpha]_D^{20} = +23.9$. Phenylmethylhydrazine yielded a crystalline derivative of D-galactose (12), m.p. and mixed m.p. 185–186° and D-glucose was identified as the phenylosotriazole, m.p. and mixed m.p. 195–196°, formed from the osazone according to the method of Hann and Hudson (9).

The presence of small amounts of galactose and glucose was thought to be most unusual and worthy of note. The fact that the amounts of these two sugars remained relatively constant through the five fractions suggested that they were not present as contaminants but as an integral part of the hemicellulose. (Although Norman (24) reported the presence of 10% galactose in oat straw, his determination was made by difference, and the mucic acid by which galactose was identified had another possible source in the unidentified uronic acid.) To our knowledge this is the first time glucose and galactose have been specifically determined and identified in hemicellulose fractions from wheat straw.

Uronic Acid Constituent

The molar ratios of methoxyl groups to uronic acid anhydride were 1.1, 1.0, 1.1., 1.4, and 0.9 in Fractions 1, 2, 4*a*, 5*a*, and 6*a* respectively.

The proximity of these ratios to unity suggested the presence of monomethoxylated hexuronic acid groups. The barium uronates (0.37 gm.), previously isolated from the hydrolysis of 10 gm. of Fraction 1, gave the following analyses:

barium 25.6%, methoxyl 4.2%, and uronic acid anhydride ($CO_2 \times 4$) 26.3%. The rather high barium content could not be reduced by reprecipitations. The molar ratio of methoxyl groups to uronic acid anhydride in the isolated barium uronates was exactly unity and this finding definitely established the presence of a monomethoxyl hexuronic acid. Hydrolysis of the barium uronate (0.24 gm.) with 2 *N* sulphuric acid (6 ml.) at 100°C. for 15 hr. and recovery of the hydrolyzate in the usual manner yielded a dark brown syrup. This syrup was dissolved in 10 ml. of water and examined by paper chromatography with a solvent system of ethyl acetate–acetic acid–water (16). Development with aniline phthalate and comparison with known sugars and uronic acids tested on the same paper indicated the presence of D-xylose and galacturonic acid. Although previous investigators (25, 36) reported the presence of a hexuronic acid in wheat straw, no evidence was reported showing it to be either glucuronic or galacturonic acid, nor was xylose shown to be associated with the uronic acid component.

Discussion

Many hemicellulose preparations are not homogeneous but are composed of several polysaccharides. The more unrefined the method of preparation, the more heterogeneous is the product. No acceptable criterion of purity of any hemicellulose material exists and neither selective precipitation by specific reagents nor fractional precipitation by alcohol and similar agents can be regarded as adequate methods. The current belief that a "pure" polysaccharide may be composed of several different sugar units has been questioned by Isherwood (15): in a recent investigation of pear cell wall polysaccharides by electrophoretic methods, he has obtained evidence that a complex polysaccharide fraction is a mixture of simple polysaccharides each consisting of a polymer of a single sugar unit. Millet and Stamm (19) fractionated aspen wood holocellulose by extraction with water followed by increasingly stronger alkaline solutions and determined the molecular weights of the fractions and their acetates by several methods. They found that the molecular weights of the various extracted materials were nearly constant and concluded that differences in solubility must be caused by chemical differences. The same conclusion was reached by Husemann (14) who determined molecular weights of xylans from wheat straw and beechwood and found all fractions to have a chain length of 150. An investigation by Thomas (34) of various hemicelluloses isolated from aspen holocellulose showed considerable variation in the uronic acid anhydride, xylan, and glucosan content of the various fractions. In the present study of wheat straw hemicelluloses, the trends in the uronic acid anhydride and pentosan contents are in accord with the conclusion that chemical differences exist between fractions. Determination of the relative proportion of sugars in the hydrolyzates yielded a more detailed picture of these differences. These differences lead to the opinion that the fractions are mixtures of hemicelluloses and that the various solvents achieved an overlapping solvent action on the various hemicelluloses in the holocellulose. However, the per-

sistence in all fractions of a small and relatively constant amount of hexoses agrees with the view of Carson and MacLay (4) that pentosans and hexosans are chemically combined. They based their conclusion on the failure of attempted fractionation of bean pod and corncob hemicellulose esters by organic solvents.

While the present investigation shows that systematic chemical differences exist between the various fractions, and therefore some fractionation has been achieved, the hemicelluloses are obviously still complex mixtures. It is regarded as highly unlikely that all fractions will have the same molecular weight. Further fractionation of the various hemicelluloses is being investigated as well as their molecular weights.

Acknowledgment

The authors wish to express their thanks to Mr. M. Carroll, student assistant, for valuable contributions in developing the liquid ammonia extraction technique.

References

1. Adams, G. A. and Castagne, A. E. Can. J. Research, B, 26: 325. 1948.
2. Anderson, E. and Krznarich, P. W. J. Biol. Chem. 111: 549. 1935.
3. Buston, H. W. Biochem. J. 28: 1028. 1934.
4. Carson, J. E. and MacLay, W. D. J. Am. Chem. Soc. 70: 293. 1948.
5. Clarke, E. P. Semimicro quantitative organic analysis. Academic Press Inc., New York. 1943.
6. Dionissiev, D. Ie. Chimie & Industrie, 43: 605. 1940.
7. Fernelius, W. C. and Bowman, G. B. Chem. Rev. 26: 3. 1940.
8. Glattfeld, J. W. E. and Macmillan, D. J. Am. Chem. Soc. 58: 898. 1936.
9. Hann, R. M. and Hudson, C. S. J. Am. Chem. Soc. 66: 735. 1944.
10. Hawthorne, J. R. Nature, 160: 714. 1947.
11. Hess, K. and Gundermann, J. Ber. 70B: 1788. 1937.
12. Hirst, E. L., Jones, J. K. N., and Woods, E. A. J. Chem. Soc. 1048. 1947.
13. Hughes, E. E. and Acree, S. F. Ind. Eng. Chem., Anal. Ed. 6: 123. 1934.
14. Husemann, E. Naturwissenschaften, 27: 595. 1939.
15. Isherwood, F. A. Abstract No. 339/11 of a communication to the 1st International Congress of Biochemistry. Cambridge. August 19-25. 1949.
16. Jermyn, M. A. and Isherwood, F. A. Biochem. J. 44: 402. 1949.
17. Keller, R. E. J. Applied Chem. (U.S.S.R.), 10: 2041. 1937.
18. Miller, C. O. and Siehrs, A. E. Proc. Soc. Exptl. Biol. Med. 29: 535. 1931.
19. Millett, M. A. and Stamm, A. J. J. Phys. & Colloid Chem. 51: 134. 1947.
20. Mitchell, R. L. and Ritter, G. J. J. Am. Chem. Soc. 62: 1958. 1940.
21. Muskat, I. E. J. Am. Chem. Soc. 56: 693. 1934.
22. Muskat, I. E. J. Am. Chem. Soc. 56: 2449. 1934.
23. Neubauer, L. G. Ph.D. Thesis, McGill. 1949.
24. Norman, G. A. Biochem. J. 23: 1353. 1929.
25. Norris, F. W. and Preece, I. A. Biochem. J. 24: 59. 1930.
26. O'Dwyer, M. H. Biochem. J. 20: 656. 1926.
27. O'Dwyer, M. H. Biochem. J. 22: 381. 1928.
28. O'Dwyer, M. H. Biochem. J. 25: 2017. 1931.
29. O'Dwyer, M. H. Biochem. J. 28: 2116. 1934.
30. Partridge, S. M. Nature, 158: 270. 1946.
31. Preece, I. A. Biochem. J. 35: 659. 1941.
32. Schulze, C. and Tollens, B. Liebigs Ann. Chem. 271: 40. 1892.
33. Somogyi, M. J. Biol. Chem. 160: 61. 1945.
34. Thomas, B. B. Paper Ind. and Paper World, 27: 374. 1945.
35. Tracy, M. V. Biochem. J. 43: 185. 1948.
36. Weihe, H. D. and Phillips, M. J. Agr. Research, 60: 781. 1940.
37. Yan, M. M. Ph.D. Thesis, McGill. 1947.

THE NEW COMPLEX COMPOUNDS OF ARGININE AND LYSINE[1]

By Alfred Taurins[2]

Abstract

The copper salts of the basic amino acids (arginine, histidine, lysine, and ornithine) are formulated as complex salts. They contain a cation (with two positive charges) consisting of a copper atom and two amino acid molecules. The anion can be a simple inorganic group, such as Cl^-, NO_3^-, $SO_4^=$. The complex copper amino acid cations form double complex compounds with anions HgI_3^- or $HgI_4^=$. The double complex salts of arginine, $[Cu(C_6H_{14}O_2N_4)_2][HgI_4]$, and lysine, $[Cu(C_6H_{14}O_2N_2)_2][HgI_3]_2$, are only slightly soluble in water and have characteristic crystal forms. They can be used for the quantitative determination of these amino acids. The copper salts of the natural amino acids are classified into four groups.

Introduction

Although the copper salts of amino acids are used for the isolation and determination of natural amino acids by different methods (2, 22), their structure and properties have been but little investigated. The copper salts of basic amino acids (arginine, histidine, lysine, and ornithine) are unusual, because they contain an inorganic anion (for example, chloride, nitrate, sulphate) in the molecule. According to previous concepts these salts were formulated as double compounds of the general type

$$2(\text{Amino acid molecule}).CuX_2.$$

Such copper salts, except those of histidine, have been known for many years. The arginine – cupric sulphate (I) and arginine – cupric nitrate (II)

$$2\ C_6H_{14}N_4O_2.CuSO_4 \qquad (I)$$

$$2\ C_6H_{14}N_4O_2.Cu(NO_3)_2 \qquad (II)$$

were isolated by E. Schulze and E. Steiger (15), and investigated by S. H. Hedin (6), W. Gulewitsch (5), and O. Riesser (14). The arginine – cupric nitrate was used later by S. P. L. Sörensen, M. Höyrup, and A. C. Anderson (17) for the isolation of arginine from protein hydrolyzates. The ornithine – cupric nitrate (III) and ornithine – cupric sulphate (IV) were isolated by M. Jaffé (7), and M. Jaffé and R. Cohn (8).

$$2\ C_5H_{12}N_2O_2.Cu(NO_3)_2.\tfrac{1}{2}H_2O \qquad (III)$$

$$2\ C_5H_{12}N_2O_2.CuSO_4.H_2O \qquad (IV)$$

The lysine – cupric chloride (V) was prepared by F. Wrede (23).

$$2\ C_6H_{14}N_2O_2.CuCl_2.2H_2O \qquad (V)$$

Although histidine hydrochloride dissolves basic cupric carbonate to form a dark blue solution of histidine – cupric chloride, this complex has not as yet been isolated in the form of crystals, presumably owing to its great solubility.

[1] *Manuscript received July 11, 1950.*
Contribution from the Organic Chemistry Laboratory, McGill University, Montreal, Que.
[2] *Lady Davis Fellow.*

In the present work it has been concluded from a study of the composition and chemical properties of the copper salts of basic amino acids that these compounds are similar to the complex compounds of copper and ammonia, or amines (for example, $[Cu(NH_3)_4]Cl_2$), and that they contain complex cations (with two positive charges) formed by a copper atom and two basic amino acid molecules. The complex cupric – amino acid cations form salts with simple anions Cl^-, NO_3^-, or $SO_4^=$, and these salts have the general formula

$$[Cu(\text{Basic amino acid})_2]^{++}X^=$$

Proof of this has been obtained by the preparation of insoluble double complex compounds formed upon addition of potassium mercuric iodide solution to a solution of cupric salt of arginine, or other basic amino acid. From previous investigations it is known that cupric – tetrammine cation reacts with potassium mercuric iodide to form two insoluble crystalline double complex salts (1, 9, 19):

$[Cu(NH_3)_4]\,[HgI_4]$	$[Cu(NH_3)_4]\,[HgI_3]_2$
Blue	Green

Similar behavior is shown by ammines of cadmium, nickel, and cobalt (19, 20), and cations of copper diethylenediamine, and copper dipropylenediamine (18).

The precipitant for several metal ammines and copper basic amino acid cations is prepared by dissolving K_2HgI_4 in water (or HgI_2 and KI in mole ratio 1: 2). It contains anions HgI_3^- and $HgI_4^=$ according to the equilibrium:

$$K_2HgI_4 \rightleftharpoons 2K^+ + HgI_4^= \rightleftharpoons 2K^+ + I^- + HgI_3^-$$

The shift of the equilibrium in favor of the $HgI_4^=$ ion occurs by the addition of an excess of potassium iodide. The solution prepared by dissolving only K_2HgI_4 is denoted in what follows as a "Reagent A", and it reacts mainly as HgI_3^-. The solution containing K_2HgI_4 + KI, denoted as a "Reagent B", reacts mainly as $HgI_4^=$ (see "Experimental").

Upon addition of "Reagent A" to a warm, dark blue cupric – lysine chloride (IX) solution and cooling to room temperature the formation of insoluble violet crystals is observed, according to the following equation:

$$[Cu(C_6H_{14}N_2O_2)_2]\,Cl_2 + 2K_2HgI_4 \rightarrow 2KCl + 2KI + [Cu(C_6H_{14}N_2O_2)_2][HgI_3]_2 \qquad \text{(VI)}$$

The crystals of cupric – lysine mercuric iodide (VI) are irregular plates which begin to crystallize from one point forming dark violet stars. It is possible to recrystallize this double complex of lysine from hot water.

The cupric – arginine chloride (XIII) solution forms crystals upon addition of the "Reagent B". The crystals are blue, and in the form of long needles or plates. Their composition is in accordance with the formula (VII). It is possible to recrystallize the double complex of arginine from hot water.

$$[Cu(C_6H_{14}N_4O_2)_2]\,Cl_2 + K_2HgI_4 \rightarrow 2KCl + [Cu(C_6H_{14}N_4O_2)_2]\,[HgI_4] \qquad \text{(VII)}$$

The most striking fact is that the copper – arginine cation prefers $HgI_4^=$ ions, and the copper – lysine cation has specific affinity for HgI_3^- ions to form insoluble double complex compounds.

The ornithine – cupric chloride (XI) solution forms with "Reagent A" an amorphous, blue precipitate, which, unlike the corresponding lysine double complex (VI), cannot be obtained as crystals from hot water. The same phenomenon was observed with a histidine – cupric chloride solution (XIV). Recrystallization of the bluish green, amorphous precipitate formed from histidine – cupric chloride and Reagents A or B yields a green amorphous substance, the composition of which does not correspond to any structure which could be predicted by a simple combination of histidine – copper cation with either HgI_3^- or $HgI_4^=$ ions.

The study of the stability and properties of the ornithine and histidine complexes is being continued.

Discussion

The structure of the basic amino acid copper complexes can be derived using the principles given by N. V. Sidgwick (16) to explain the formation of complex compounds in terms of the electronic theory of valence.

When a cupric cation, Cu^{++}, reacts with two amino acid anions (for example, glycine anion, $H_2N–CH_2–COO^-$), it forms four bonds with two carboxylic and two α-amino groups. The resultant charge of the copper atom in the complex is zero, because two positive charges of the cupric cation are neutralized by two negative charges of two oxygen atoms of the carboxylic anions. Two additional co-ordinate covalent (semipolar double) bonds are formed between the copper atom and two amino groups by sharing of two electron pairs between the copper atom and two nitrogen atoms. But the formation of such a bond does not produce any additional charges on the copper atom. The resultant charge of the atoms surrounding the copper atom is zero; two nitrogen atoms form co-ordinate covalent bonds with the copper atom, each contributing a shared electron pair and acquiring two positive charges; two oxygen atoms form two bonds, acquiring two electrons from the copper atom and obtaining two negative resultant charges; the positive and negative charges neutralize each other.

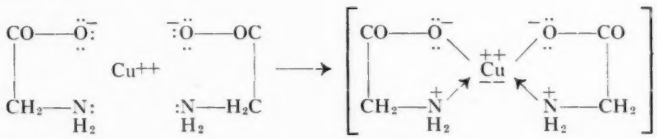

The formation of two positive charges of cupric basic amino acid complex cation is due to the nitrogen atoms of the remaining basic groups of amino acids, as shown in the following equations demonstrating the formation of the complex compounds.

The formation of *lysine – copper chloride complex salt* (*IX*) is observed by treatment of a solution of lysine monohydrochloride (VIII) with freshly prepared basic cupric carbonate, $Cu(OH)_2.CuCO_3$. This carbonate is a weak base which does not react upon the ϵ-ammonium chloride group of lysine monohydrochloride and does not convert it into the free ϵ-amino group.

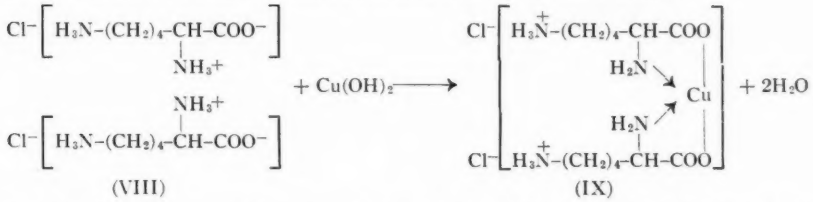

(VIII) (IX)

In a similar way ornithine monohydrochloride (X) reacts with basic cupric carbonate and forms the *ornithine – copper chloride complex salt* (*XI*)

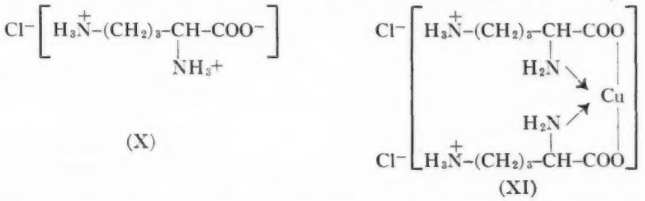

(X) (XI)

The formation of arginine – copper chloride complex (XIII) occurs in a similar manner and the basic cupric carbonate does not convert the guanidinium chloride group

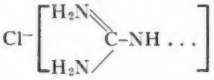

of arginine hydrochloride (XII) into the free guanidine group. Therefore the two positive charges of (XIII) are located on nitrogen atoms of the guanidinium groups.

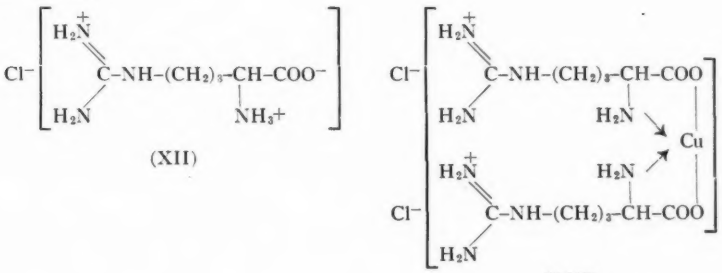

(XII) (XIII)

The positive charges of a histidine – copper chloride complex (XV) should be located at nitrogen atoms of the imidazolium group similarly as in histidine monohydrochloride (XIV).

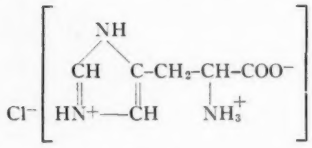

(XIV)

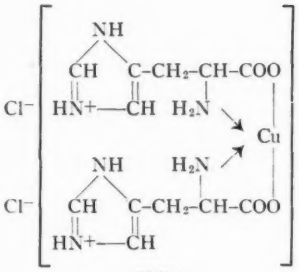

(XV)

(In guanidinium and imidazolium groups, positive charges are not actually located at definite N atoms since these groups resonate among different structures.)

Types of Copper Salts of Amino Acids

Considering the 25 naturally occurring amino acids which contain different side chains and groups, evidence exists for the following four main groups of their copper salts.

The *first group* includes the copper salts of *monoamino monocarboxylic acids* with unpolar side chains (glycine, alanine, valine, leucine, isoleucine, phenylalanine, and proline). These dark blue salts were early recognized as inner complex compounds, in which copper is bound by two covalent and two coordinate covalent links in two five-membered chelate rings (3, 4, 10, 11, 12).

The *second group* contains the copper complex salts of *monoamino monocarboxylic acids* with polar side chains (serine threonine, tyrosine, hydroxyproline, tryptophane, methionine, cystine, and cystein). This group is closely related to the first one, being also inner complex compounds, but differing from the first group in the ability to form additional linkages with copper atoms by interaction of the polar groups of these amino acids. The copper salts of this group need further investigation of their structures.

The *third group* includes the copper complex salts of *monoamino dicarboxylic acids* (aspartic and glutamic acids), containing anions formed by two amino acid molecules and a copper atom which are linked together in the inner complex of two five-membered chelate rings; the second copper atom is in the outer sphere bound by ionic linkage. The empirical formula of the copper salt of aspartic acid is $CuC_4H_5NO_4$, but according to P. Pfeiffer and H. Werner (13) the correct structure of this compound is $Cu(C_5H_5NO_4)_2$ Cu or (XVI):

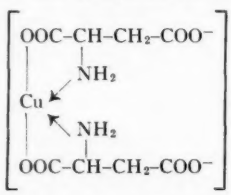

(XVI)

Pfeiffer and Werner proved this structure by the preparation of sodium and barium salts of copper-aspartic complex.

The *fourth group* consists of the complex copper salts of *basic amino acids* (arginine, histidine, lysine, and ornithine), previously discussed in detail.

Quantitative Determination of Arginine and Lysine in the Form of the New Complex Compounds

The double complex compounds of arginine (VII) and lysine (VI) are formed very easily in the form of crystals which have very small solubility in cold water. They have unusually high molecular weights in comparison with those of the amino acids. The complex of arginine (VII) has a molecular weight 1120.3 with the arginine content only 31.1%, while the molecular weight of the lysine complex (VI) is 1518.7, with a lysine content of only 19.25%. All these factors strongly suggest the use of these complex compounds for the quantitative determination of arginine and lysine.

Experimental

K_2HgI_4 reagent.—For the precipitation of lysine – copper complex the *Reagent A* was used. It was 1/5 molar and contained 15.74 gm. K_2HgI_4 in 100 ml. of solution, prepared by dissolving 6.65 gm. KI and 9.09 gm. HgI_2. For the precipitation of 1 gm. lysine monohydrochloride, 27.4 ml. of Reagent A was needed (K_2HgI_4 mol. wt. = 786.48; lysine hydrochloride, mol. wt. = 182.59).

For the precipitation of arginine–copper complex 1/5 molar *Reagent B* was used, containing 15.74 gm. K_2HgI_4, and an excess of 5 gm. KI in 100 ml. of solution. To precipitate 1 gm. arginine monohydrochloride 11.9 ml. of Reagent B was required (arginine hydrochloride mol. wt. = 210.61).

Preparation of copper – amino acid complexes.—To a solution of 2.00 gm. amino acid monohydrochloride in 100 ml. water a freshly prepared basic cupric carbonate was added in small excess and heated to boiling. After cooling, the dark blue solution was filtered and diluted to the desired concentration. The solutions of copper – amino acid complexes did not contain any excess of free amino acids.

Preparation of the double arginine complex (VII).—A solution of copper – arginine chloride complex was prepared from 2.00 gm. of arginine hydrochloride, diluted with water to 500 ml., and heated to 95°C. To this dark blue hot solution 25 ml. of Reagent B was added and the whole allowed to cool slowly. The formation of long blue crystals was observed. They were filtered off, washed with a small amount of water, and dried. Yield: 5.28 gm. (99.2%). M.p. 215–216°C.

Analysis of the arginine complex.—Carbon, hydrogen, and nitrogen were determined by micromethods. To estimate copper, mercury, and iodine the complex was decomposed with dilute sulphuric acid, and the copper and mercury

precipitated with hydrogen sulphide as CuS and HgS, and then separated by the usual methods (21). Iodine was estimated volumetrically in the filtrate (21). Calc. for $C_{12}H_{28}N_8CuHgI_4$ (mol. wt. = 1120.27): C, 12.87; H, 2.52; N, 10.00; Cu, 5.67; Hg, 17.91; I, 45.32. Found: C, 12.89; H, 2.63; N, 9.90; Cu, 5.48; Hg, 17.91; I, 44.96.

Limit of the determination of arginine.—The copper – arginine chloride solution was prepared from 1.0000 gm. of *l*-arginine hydrochloride and diluted to 100 ml. From this solution several dilute solutions were prepared as shown in Table I. To 5 ml. of each solution 1 ml. of Reagent B was added and the formation of crystals of the double complex (VII) observed. In the most dilute solution (No. 6), containing 0.1 mgm. of arginine hydrochloride in 1 ml. of solution, a precipitate was formed after 24 hr. From solution 5, containing 0.25 mg. of arginine hydrochloride in 1 ml., long needles of the complex were formed in 1–2 hr. If only 1 ml. of each solution is tested with 0.2 ml. of Reagent B the formation of crystals requires more time. These experiments show that it is possible to detect 0.1 mgm. of arginine monohydrochloride in 1 ml. of solution (Table I).

TABLE I

DETERMINATION OF ARGININE

No.	Arginine-HCl in 1 ml., gm.	Precipitation of crystals from 5 ml. solution + 1 ml. reagent	Precipitation of crystals from 1 ml. solution + 0.2 ml. reagent
1	0.01	1/2–1 min. from hot soln.	
2	0.002	1–2 " " " "	20–25 min. from hot soln.
3	0.001	2–3 " " " "	45–60 " " " "
4	0.0005	1/2–1 hour from cold soln.	1–2 hour from cold soln.
5	0.00025	1–2 hr, " " "	2–3 " " " "
6	0.0001	12–24 " " " "	24 " " " "

Preparation of the lysine complex (VI).—To a hot solution (190 ml.) prepared from 2.000 gm. lysine monohydrochloride and a small excess of basic cupric carbonate, 60 ml. of K_2HgI_4—Reagent A—was added. By slow cooling, the formation of compact crystals in the form of dark stars was observed. After 48 hr. the crystals were filtered off, washed with a small amount of water, and dried in a vacuum desiccator. Yield 8.20 gm. (the theoretical amount 8.318 gm.), M.p. 217–218°C.

It turns black by heating at 110°C., but regains its original color on cooling. The complex (VI) has the same composition and properties when prepared from either *dl*-lysine or L(+)-lysine.

Analysis of the lysine complex was conducted using methods similar to those outlined for the arginine complex. Calcd. for $C_{12}H_{28}N_4O_4CuHg_2I_6$ (mol. wt. = 1518.7): C, 9.49; H, 1.86; N, 3.69; Cu, 4.19; Hg, 26.42; I, 50.14. Found: C, 9.66; H, 2.05; N, 3.72; Cu, 4.05; Hg, 25.96; I, 49.78.

Limit of the qualitative determination of lysine is 0.1 mgm. lysine monohydrochloride in 1 ml. of solution with 0.2 ml. of Reagent A. At such dilution the formation of crystals can be observed only after 24 hr.

Acknowledgment

The author wishes to thank Mr. J. F. Eagen, Microanalytical Laboratory, National Research Council, Ottawa, for the microanalyses of carbon, hydrogen, and nitrogen.

References

1. ANDERLINI, F. Gazz. chim. ital. 42(I): 321. 1912.
2. BRAZIERS, M. A. B. Biochem. J. 24: 1188. 1930.
3. BRUNI, G. Z. Elektrochem. 11: 93. 1905.
4. BRUNI, G. and FORNARA, C. Atti reale accad. Lincei, [5], 13 (II): 26. 1904.
5. GULEWITSCH, W. Z. physiol. Chem. 27: 178. 1899.
6. HEDIN, S. H. Z. physiol. Chem. 20: 186. 1895; 21: 155. 1895.
7. JAFFÉ, M. Ber. deut. chem. Ges. 10: 1926. 1877; 11: 406. 1878.
8. JAFFÉ, M. and COHN, R. Ber. deut. chem. Ges. 21: 3464. 1888.
9. JÖRGENSEN, S. M. J. prakt. Chem. 2(2): 347. 1870.
10. LEY, H. Z. Elektrochem. 10: 954. 1904.
11. LEY, H. Ber. deut. chem. Ges. 42: 354. 1909.
12. LEY, H. and HEGGE, H. Ber. deut. chem. Ges. 48: 70. 1915.
13. PFEIFFER, P. and WERNER, H. Z. physiol. Chem. 246: 212. 1937.
14. RIESSER, O. Z. physiol. Chem. 49: 20. 1906.
15. SCHULZE, E. and STEIGER, E. Z. physiol. Chem. 11: 43. 1904.
16. SIDGWICK, N. V. J. Chem. Soc. 433. 1941.
17. SÖRENSEN, S. P. L., HÖYRUP, M., and ANDERSON, A. C. Z. physiol. Chem. 56: 44. 1911.
18. SPACU, G. and SUCIU, G. Z. anal. Chem. 77: 334. 1929; 78: 329. 1929; 92: 247. 1933.
19. TAURINS, A. Z. anal. Chem. 97: 27. 1934.
20. TAURINS, A. Z. anal. Chem. 101: 357. 1935.
21. TREADWELL, F. P. and HALL, W. T. Analytical chemistry. Vol. 2. 7th ed. John Wiley and Sons Inc., New York. 1928, pp. 172, 570.
22. WIELAND, TH. and FREMERY, H. Ber. deut. chem. Ges. 77: 234. 1944.
23. WREDE, F. Z. physiol. Chem. 203: 162. 1931.

FLOCCULATION IN SUSPENSIONS OF LARGE PARTICLES[1]

By C. E. Hubley[2, 3], A. A. Robertson[2, 4], and S. G. Mason

Abstract

Based upon an assumed mechanism of particle aggregation by shear-induced interparticle collisions, a new method of studying flocculation in suspensions of large particles is described, and representative results obtained with cellulose-fiber suspensions are presented. The method consists in subjecting the suspension to a reproducible condition of shear motion and analyzing the fluctuations in optical transmission coefficient electronically. An approximate statistical theory is presented on the basis of which a flocculation index (σ/N_0) appropriate to the method is proposed. The index is a function of both the number and size of the aggregates. The flocculation index was found to decrease with increasing rate of shear and decreasing fiber length. The effect of concentration and of additives was investigated. Alternative experimental techniques are outlined and limitations to the present method are pointed out.

Introduction

Particle aggregation, or flocculation, in liquid suspensions of large particles possessing negligible Brownian movement, is a phenomenon of fundamental and practical importance. Few systematic studies of this phenomenon, however, are reported in the literature, the principal reason, it would appear, being the experimental difficulty of carrying out direct quantitative measurements of the degree of dispersion in such systems. In conventional colloidal sols flocculation occurs spontaneously, after destruction of the protective action, from collisions promoted by Brownian motion which allow the interparticle attractive forces to come into play. Such flocculation is usually sharply defined. By contrast, aggregation of large particles, by interparticle attraction, mechanical entanglement (12), or special mechanisms such as interfacial tension (1, 4, 7, 10, 11), is ill-defined. In addition, it is invariably complicated by a number of factors such as the lack of reproducible particle motion, sedimentation, etc., especially in dilute suspensions where disconnected particle structures are formed.

The most successful experimental methods, apart from visual observations and particle counts which at best are applicable only to systems whose primary particles are of uniform size and well defined shape, involve measurements of the thixotropy (9), yield point (10), or the sedimentation volume (4, 15). The rheological methods find their principal application to relatively concentrated suspensions in which connected structures, as, for example, in pastes, greases, and gels, are formed; in this connection, interest in flocculation is centered upon its effect on the rheological properties of the system. Sedimentation methods have been used in dilute suspensions, but the results are often inconclusive.

[1] *Manuscript received July 20, 1950.*
Joint contribution from Chemistry Department and Pulp and Paper Research Institute of Canada, McGill University, Montreal, Que.
[2] *Holder of Studentships under the National Research Council of Canada.*
[3] *Present address: Defence Research Board of Canada, Ottawa, Ont.*
[4] *Present address: Pulp and Paper Research Institute of Canada.*

This communication deals with a method developed to study aggregation phenomena in cellulose–water suspensions. It is believed that this method can, with suitable modification, be adapted to other systems. In this investigation, interest was directed towards a study of factors influencing localized fluctuations in concentration which, in the process of making paper from the fiber suspensions, persist and give the paper a mottled appearance when viewed by transmitted light.

Principle of the Method

The essential idea of the method is to create reproducible conditions under which the particles can undergo collisions. This is done by subjecting the suspension to simple shear motion. Under these conditions, assuming independent particle movement, the frequency f of two-body collisions per unit volume is given by (12)

$$f = kGN^2v, \tag{1}$$

where N = the number of particles per unit volume,
G = the rate of shear,
v = the average volume per particle,
k = a factor determined by the size distribution and shape of the particles. For a monodisperse system of spheres, $k = 8/\pi$.

A mechanism is thus provided whereby the particles are brought into contact, and, if conditions are favorable, can adhere to form nuclei of flocs which can grow by further collisions. The growing flocs will be subjected to disruptive stresses arising from the shearing action of the fluid increasing as G increases. According to this simple mechanism, therefore, the motion allowing the flocs to form will also tend to destroy them. If sufficient time is allowed, one might therefore expect the establishment of a dynamic equilibrium between floc formation and floc destruction. One would further expect the position of equilibrium to shift in the direction of higher dispersion as G is increased. Evidence of the general validity of this line of reasoning is presented later.

Fluctuations in Concentration

The local fluctuations in concentration are measured by passing a narrow beam of light through a suspension contained between concentric cylinders of the Couette system in which the outer cylinder is rotated; in this way the suspension is scanned at a rate equal to half the peripheral speed of the moving cylinder. The emergent beam impinges upon a photoelectric cell whose output varies erratically with time as a result of fluctuations in local concentration caused by aggregation. The instantaneous transmission is related to the local concentration by an equation of the type

$$T = e^{-\kappa c}, \tag{2}$$

where T = the transmission coefficient of the suspension,
c = the average concentration in the field of the light beam,
κ = a constant determined by the scattering coefficient of the particles and the distance between the cylinders.

The photocell output consists of a mean d-c. component, characteristic of the average transmission level of the suspension, with a superimposed a-c. current of wave form dependent upon the particle size distribution, and of frequency dependent upon the particle number and scanning speed.

Approximate Theory of Measurement of Fluctuations

In this section the principles of computing the degree of flocculation from the fluctuations of T are outlined. A rigorous theoretical treatment of the statistical theory of the fluctuations involved, analogous to the theory of random noise (13, 14), will not be attempted. Instead the discussion is restricted to an approximate treatment sufficient for the present purpose.

It is assumed that the distribution of transmission levels T about the time-average value $\overline{T}$ is Gaussian, i.e.,

$$p(x) = \int_x^\infty \frac{1}{\sigma\sqrt{2\pi}} e^{-x^2/2\sigma^2} dx , \qquad (3)$$

where $x = (T - \overline{T})$,
$p(x)$ = probability of a fluctuation exceeding x,
and σ = r.m.s. or standard deviation of the fluctuations.

If the fluctuations are described by Equation (3), it is clear that σ is a measure of the amount of aggregation. A number of methods of determining σ experimentally were considered and are described below.

A. Pulse Counting

In the pulse-counting method (Fig. 1*A*), a count is registered on a scaler each time the photocell output crosses the discrimination level in the downward (decreasing T) direction. The discrimination level is varied over the entire range of fluctuations, and a distribution function of pulse counts per unit distance of suspension scanned is thereby obtained.

If it is further assumed that the *sequence* of pulses is random, the probability that a fluctuation exceeding x is immediately followed by one less than x is $p(x)\,[1 - p(x)]$.

Thus the pulse-counting rate $N(x)$ per unit distance scanned may be written

$$N(x) = N_0 p(x)[1 - p(x)] \qquad (4)$$

At the time-average transmission level, Equation (4) reduces to $N(0) = N_0/4$. Thus the constant N_0 should equal four times the maximum counting rate.

Two quantities σ, which may be regarded as a statistical measure of the size of the particle aggregates, and N_0, which is related to the average number of particles per unit volume, can thus be computed from the pulse-count distribution curve. Flocculation of an initially dispersed suspension should, on this basis, yield a high σ and a low N_0. Both quantities may be regarded as measures of the amount of flocculation. The quantity σ/N_0 has been arbitrarily chosen as an over-all index determined by this method.

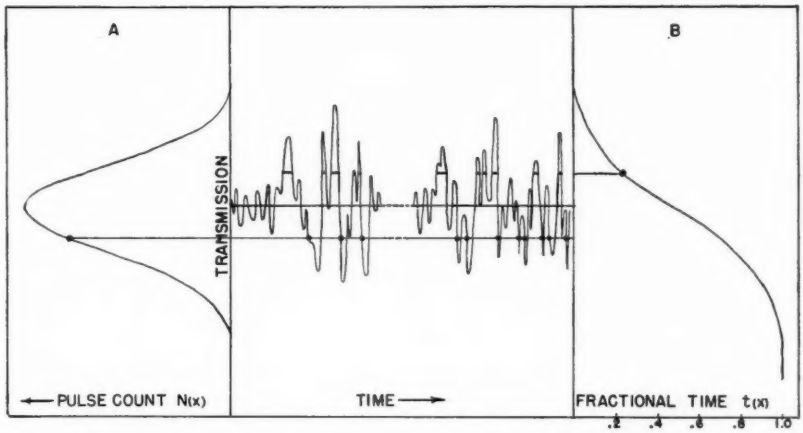

FIG. 1. *Fluctuations in transmission of a suspension due to flocculation. The distribution of transmission levels is shown in two ways:*

(A) The distribution of the number of pulse counts $N(x)$ per unit length of scanning at the transmission level corresponding to x;

(B) The distribution of the time fraction $t(x)$ during which the transmission level corresponding to x is exceeded.

B. Time Integration (Fig. 1*B*)

This analysis, similar in principle to that employed by Goetz *et al.* (8) in measuring the graininess of photographic emulsions, is related to Method *A*, but differs in the manner of obtaining the distribution curve. A chronometric device, described later, measures the time the transmission is above, or alternatively below, selected transmission levels. The fraction of time $t(x)$ during which the transmission level exceeds the deviation x, from the approximate theory given above, corresponds to $p(x)$. Thus from the distribution curve $t(x)$, it should be possible to compute a value of σ which should be the same as that given by Method *A*. Reasonably good agreement was found between the values obtained by the two procedures. It should be noted that the time-integration method, however, provides only a single index of flocculation.

C. Current-time Integration

An integration may be carried out at various discrimination levels using a current-integrating device of high time constant. In this method the quantity $\frac{1}{t}\int^{t} (T - T_0)\, dt$ for $T > T_0$, where t is time, is determined at various levels of T_0 and an appropriate distribution function is calculated. A simple variation of this method is to integrate at the time-average transmission level $\bar{T}$, thus obtaining an index which is directly proportional to σ.

D. R.M.S. Fluctuations in Transmission.

This method has been successfully used for determining the uniformity of paper by high-speed scanning with transmitted light (3, 6). The photocell output is passed through an a-c. amplifier and the r.m.s. output is determined on an a-c. voltmeter. This method measures σ directly.

E. Average Transmission

It is readily shown from an analysis of Equation (2) that fluctuations in concentration will increase the time-average transmission level by an amount depending upon the degree of particle aggregation. This effect is illustrated in some of the results presented later.

All the above methods were tried. Only the first two yielded sufficient sensitivity in the systems studied. Of these the pulse-counting technique was found to be the more suitable because it provides a value of N_0. It is possible, however, that the other methods, several of which have the advantage of greater simplicity, may be applicable to other systems.

Experimental Part

The suspension is held in the Couette system (Fig. 2) between the concentric vertical cylinders *A* (8.18 cm. I.D.) and *CBD* (6.42 cm. O.D.). The outer

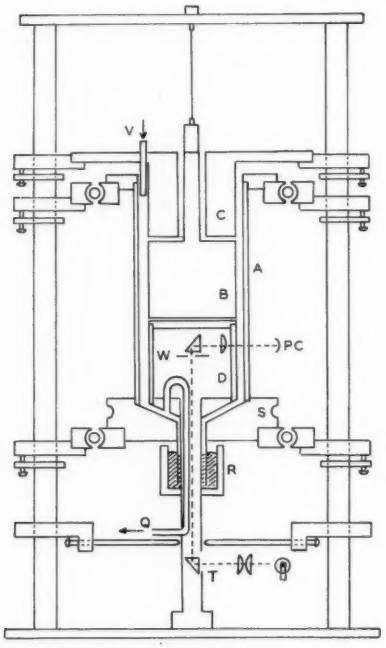

FIG. 2. *Mechanical and optical components of the apparatus.*

cylinder A rotates on bearings, thus subjecting the suspension to an approximately constant shear rate. The cylinders taper sharply at the bottom to concentric shafts, the inner one supporting a mercury seal R.

In the original design, provision was made to suspend cylinder B by a torsion wire so that it might revolve freely between guard cylinders C and D and thus form a Couette viscometer. However, in all experiments described here B, C, and D are stationary. The main portion of cylinder D is of glass and contains part of the optical system.

In the majority of the experiments performed, the particles tended to settle out. To overcome this, the suspension was drawn continuously from the bottom through the tube Q by a midget pump and reintroduced at V. The pump was regulated to the lowest speed at which sedimentation was avoided. It might be objected that this introduced an unknown amount of shear over that computed from the speed of rotation of A. Experience showed, however, that at low pumping rates the amount of flocculation was not sensibly affected in the systems employed.

The outer cylinder is rotated by a belt drive at S connected to a variable-speed motor with a stabilized voltage input. The speed of rotation may be varied and closely controlled from 0 to 400 r.p.m., thus producing rates of shear from 0 to 200 sec.$^{-1}$

The optical system consists of an exciter lamp, two prisms and three lenses so placed that a beam of light enters the central shaft at T, is directed upwards through the shaft and inner cylinder, and is reflected and focused in a narrow cone through the suspension onto a photocell. The size of the beam is controlled by a diaphragm at W to a maximum cross section of 1 sq. mm. The lamp is powered by storage batteries and its intensity may be varied by means of a series rheostat.

A block diagram of the electronic equipment is shown in Fig. 3. The photocell circuit together with the discriminator, pulse-counting, and calibration circuits are outlined in Fig. 4. The photocell output is amplified in T1. T2 is a square-wave generator which produces a standard pulse whenever the signal voltage exceeds a value selected by the discriminator control P3. The pulses are amplified in T3 and counted by an electronic scaling unit and register. Thus a pulse is counted whenever a floc of appropriate size enters the light beam; the minimum size of floc counted is controlled by the discriminator setting.

In setting up the apparatus for a run, the various electrical circuits are turned on for three hours before calibration to avoid subsequent drift. The potentiometer is used to adjust the maximum potential of the standard signal source to an arbitrary value of 3.14 v. The corresponding deflection on the vacuum-tube voltmeter is noted. The exciter-lamp intensity is adjusted so that the same deflection is produced by the photocell output when the apparatus contains water only.

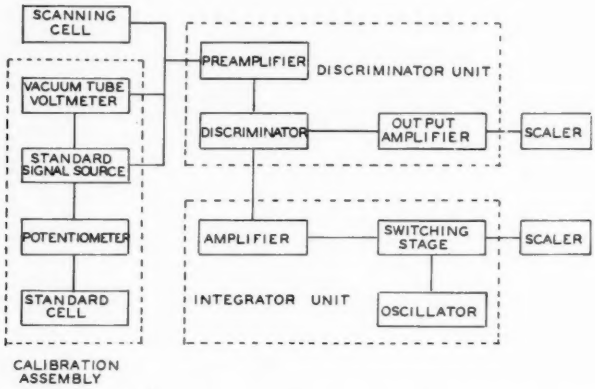

FIG. 3. *Block diagram of pulse analysis showing the relation of the pulse-counting and time-integration units.*

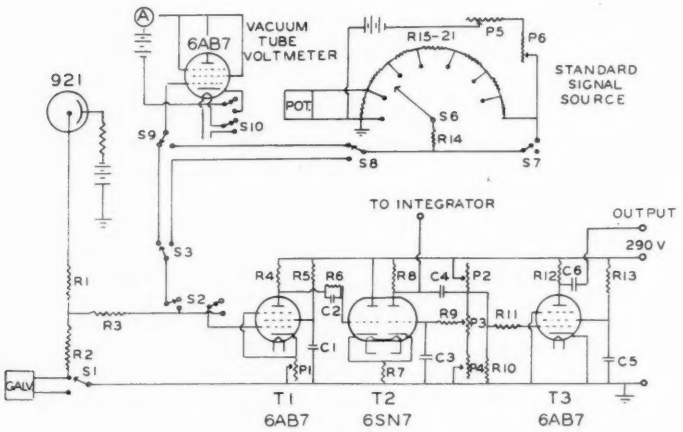

FIG. 4. *Pulse-counting circuit.*

The discriminator is calibrated by applying potentials from the standard signal source to the grid of the preamplifier T1. These signals are known fractions of the maximum potential, and the discriminator setting at which each just registers on the scaler is determined. In this manner the discriminator is calibrated in terms of transmission levels.

The suspension is introduced into the apparatus, the circulation system is started, and the outer cylinder rotated. For pulse counting, the data recorded are:

(*a*) The average current in the photocell circuit as read on a damped galvanometer.

(*b*) The pulse counts registered during timed intervals (one or two minutes) at a sufficient number of transmission levels to define a pulse-distribution curve. These data are converted to pulse counts per centimeter scanned. The mean speed of scanning is taken to be one-half the peripheral velocity of the outer cylinder. The lamp intensity is maintained at a constant value with the aid of a monitor photocell.

The time-integration unit (Fig. 5) consists of an amplifier, a switching stage, an oscillator, and a scaler-register. The output of the discriminator T2 (Fig. 4) is amplified and fed to the switching stage. The arrangement is such that the oscillator output (60 to 500 c.p.s.) is fed to a scaler whenever the photocell current exceeds the discrimination level. Alternatively the circuit may be altered by a switch so that the oscillations are counted when the transmission level is below the level of discrimination.

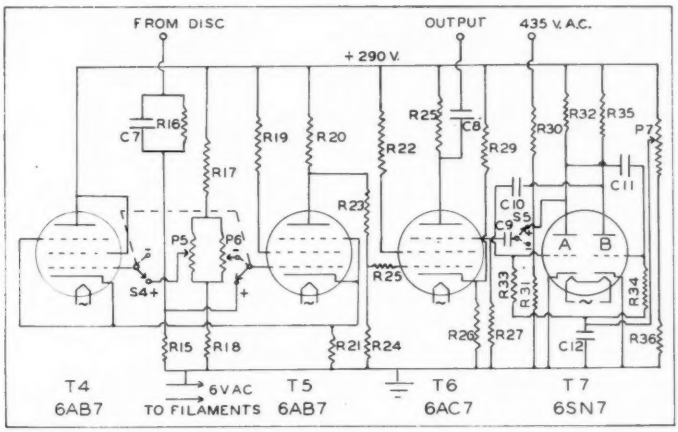

FIG. 5. *Time-integration circuit.*

The operation of the apparatus was checked by scanning a strip of processed motion-picture film affixed to the revolving cylinder. In one case the photocell output was recorded on an Esterline–Angus recording galvanometer while the film was scanned at 4 cm. per min. Pulse-counting and time-integration data were obtained by analyzing the graph and were compared with data obtained at 200, 550, and 850 cm. per min. by the procedure proposed for the examination of suspensions.

The data were found to agree within experimental error. Figs. 6 and 7 show the results obtained by both methods. It is not to be expected that pulse-counting and time-integration should give comparable results in this case, since the distribution of transmission levels cannot be considered random.

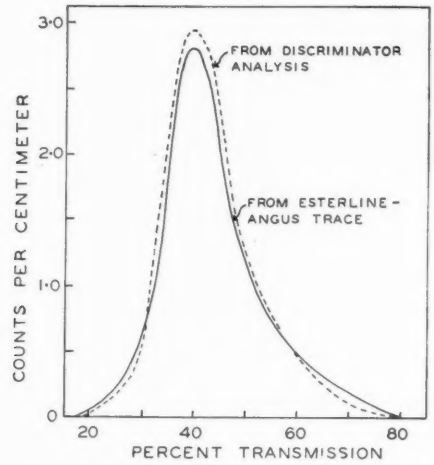

FIG. 6 *Comparison of pulse-count distribution with data obtained from recorder trace.*

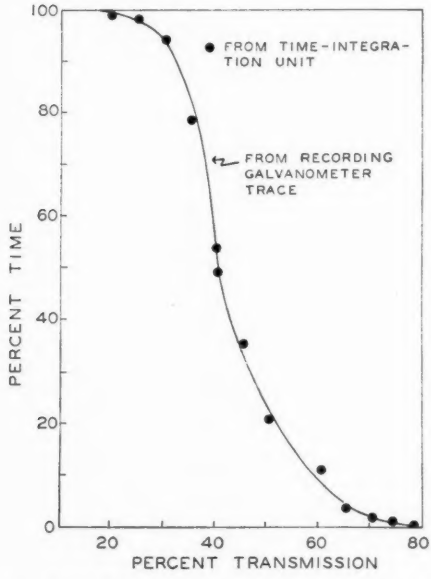

FIG. 7. *Comparison of data by time integration with that computed from recorder trace.*

Results

Comparison of Pulse-Counting and Time-Integration

The assumption that the time-integration and pulse-counting methods should reveal similar distributions was tested using a dilute suspension of wood-pulp "fines". The particles were prepared by screening a "beaten" pulp stock and collecting the pass 200 mesh fraction. This consists of irregularly shaped fiber debris less than 0.2 mm. in length. Similar samples were used in most of the experiments described below.

The experiment was conducted so that pulse-counting and time-integration data were obtained simultaneously. Curves comparing the results obtained by the two methods are presented in Fig. 8. The pulse counts per centimeter of suspension scanned are plotted as a function of the transmission level to give a pulse-distribution curve. The time-integration curve is obtained by plotting the product, $N_0 t(x)[1 - t(x)]$. The factor N_0, obtained by pulse-counting, is included so that the distributions may be compared graphically.

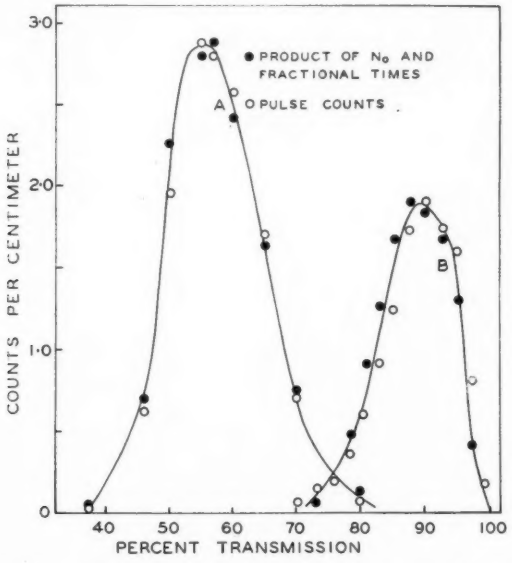

FIG. 8. *Comparison of distribution curves obtained by pulse counting and time integration. The suspensions scanned were bleached sulphite fines*
(A) 0.081 gm. per 100 ml. at 13 sec.$^{-1}$
(B) 0.033 gm. per 100 ml. at 17 sec.$^{-1}$

It is considered that the data are sufficiently in agreement to confirm the suggested relation. In view of this agreement, which was repeatedly confirmed, it appears that the time-integration method does not provide any information that is not given by the pulse-counting technique. Subsequent experiments therefore were carried out using pulse-counting only.

The same data (Fig. 8, *A*) may be used to illustrate the method of calculating σ from the experimental data. For present purposes, it has been found convenient to define σ as the spread of the experimental curve relative to the normalized distribution function,

$$N = N_0 p(s)[1 - p(s)]$$
$$= N_0 \left[\int_{-\infty}^{s} \frac{1}{\sqrt{2\pi}} e^{-s^2/2}\, ds \right] \left[\int_{s}^{\infty} \frac{1}{\sqrt{2\pi}} e^{-s^2/2}\, ds \right], \qquad (5)$$

where $p(s)$ is the probability of a deviation exceeding s when the standard deviation is unity. The values of Equation (5) for several representative values of s are determined using probability function tables. The spread of the experimental curve at these ordinate (N) values is measured. Then σ = experimental spread/2s. Several values of σ are thus obtained for each curve and these are averaged. The operations are shown in Table I.

TABLE I

CALCULATION OF THE FLOCCULATION INDEX

s	$p(s)$	$N_0[p(s)][1 - p(s)]$ (observed N_0 = 11.7)	Observed spread, % transmission	σ spread/2s
0.40	0.6559	33.8	6.5	8.1
0.80	0.7881	25.0	12.8	8.0
1.20	0.8849	15.3	18.0	7.5
1.60	0.9452	7.7	25.9	8.1
2.00	0.9773	3.3	32.8	8.2
		Average σ = 8.0		
		Flocculation index σ/N_0 = 0.68		

The curves in most instances deviated in shape from the theoretical curve. At concentrations above 0.1 and below 0.04 gm. per 100 ml. particularly, they were markedly skewed. However, it was found that wh e curves were analyzed by using spreads consistent values of σ were o

Variation of Shear Rate

The existence of a dynamic equilibrium was indicated by experiments in which pulp suspensions were subjected to varying rates of shear. It was found that floc-particle equilibria were quickly attained in such systems. The equilibrium moreover could be reproduced repeatedly by restoring a given rate of shear even though the equilibrium was disturbed in the interval. Results demonstrating this reproducibility are shown in Fig. 9.

A number of runs were made with suspensions of bleached sulphite fines to determine the effect of change in the rate of shear on the degree of flocculation. The limit to which the shear rate could be increased, in the apparatus described, without inducing turbulence is doubtful. It is, however, considered that flow is laminar below G = 32 sec.$^{-1}$ and that any appreciable centrifuging action is absent.

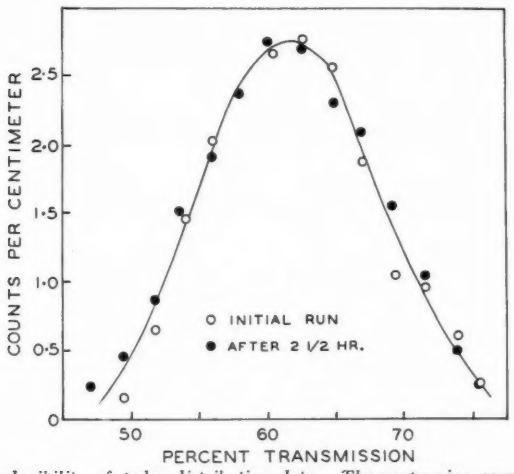

FIG. 9. *Reproducibility of pulse distribution data. The suspension scanned was bleached sulphite fines at 0.0815 gm. per 100 ml. Two sets of data were recorded 2.5 hr. apart at a shear rate of 16 sec.*$^{-1}$ *During the interval the suspension was sheared at 56 sec.*$^{-1}$

A typical set of distribution curves obtained at various values of shear rate G, and the corresponding values of σ, N_0, and σ/N_0 are shown in Figs. 10 and 11 respectively. It will be noted that there is an increase in N_0 and a decrease in σ as G increases, showing a change in the degree of flocculation in the direction anticipated.

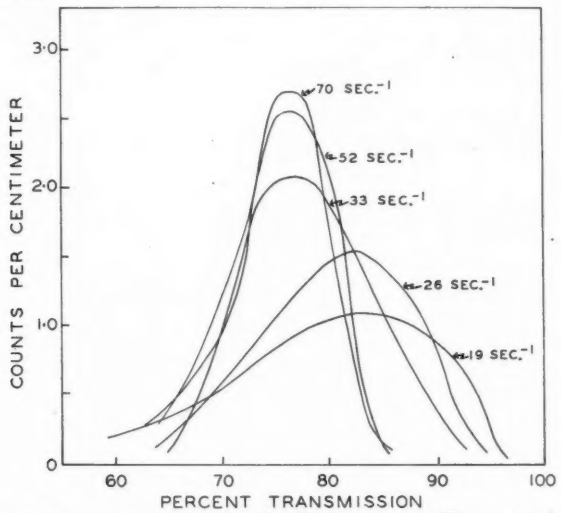

FIG. 10. *Effect of shear rate on pulse distribution curves. The suspension scanned was 100/200-mesh bleached sulphite pulp at 0.04 gm. per 100 ml. concentration. The shear rates were 19, 26, 33, 52, and 70 sec.*$^{-1}$ *and the corresponding flocculation indices were 2.66, 1.35, 0.925, 0.575, and 0.470.*

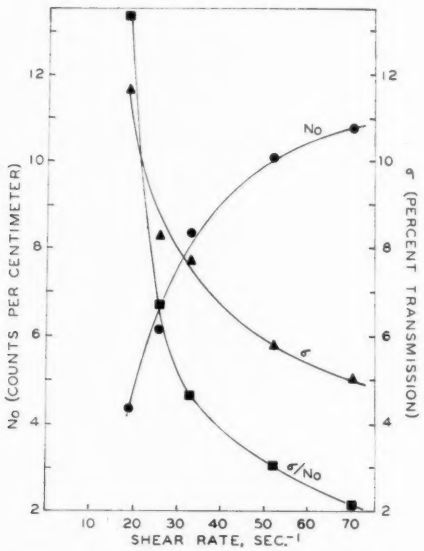

FIG. 11. *Effect of shear on pulse-distribution curve values. The variation of* σ, N_0, *and* σ/N_0 *are shown.*

Concentration Effect

Fig. 12 indicates the results obtained by varying the concentration of pulp-fines suspensions over a 10-fold range (0.018 to 0.167 gm. per 100 ml.) at a constant shear rate of 13 sec.$^{-1}$ Analysis of the distribution curves is reported in Table II. It is noticed that as the concentration is increased, the ratio σ/N_0 passes through a maximum. This behavior is not unexpected and the reason for it is discussed qualitatively below.

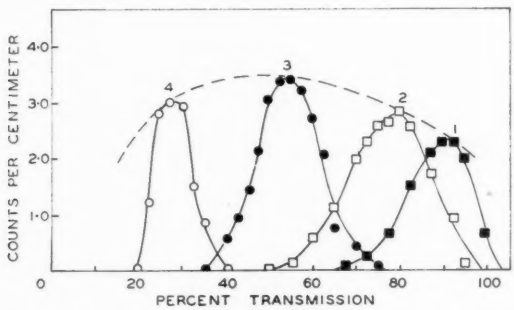

FIG. 12. *Effect of consistency on pulse-distribution curves for bleached sulphite fines at a shear rate of 13 sec.*$^{-1}$ *The concentrations were 0.018, 0.041, 0.081, and 0.167 gm. per 100 ml.*

TABLE II

CONSISTENCY AND THE FLOCCULATION INDEX (FIG. 12)

Concentration, gm./100 ml.	N_0, counts/cm.	σ	σ/N_0
0.167	12.0	4.7	0.392
0.0815	13.7	8.2	0.600
0.041	11.0	10.4	0.941
0.018	9.3	8.1	0.870

Variation of Fiber Length

If it is assumed that mechanical entanglement is a factor promoting the stability of flocs, it would be expected that increased fiber length should result in increased flocculation. Experiments were therefore carried out in which the shear was maintained constant and the degree of flocculation was varied by the addition of longer fibers. The shear rate chosen was 16 sec.$^{-1}$; the consistency was maintained constant at 0.08 gm. per 100 ml. but the proportion of 48/100-mesh pulp (av. length 0.7 mm.) and pass-200-mesh "fines" (< 0.2 mm. length) was varied. The results are illustrated in Fig. 13 and show clearly the increased flocculation index produced by the presence of longer fibers. It should be pointed out, however, that the substitution of small particles by larger ones leads to a reduction of the coefficient κ in Equation (2), and thus to changes in the average transmission level $\bar{T}$ not solely attributable to changes in the degree of flocculation.

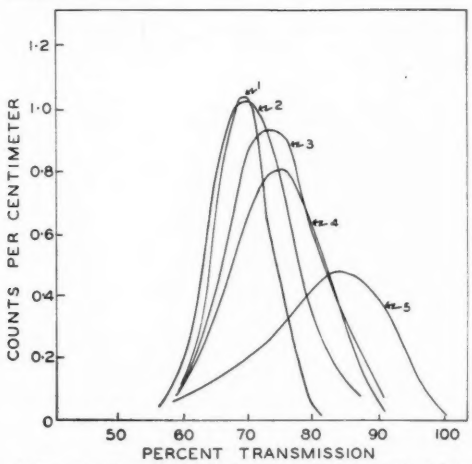

FIG. 13. *Effect of fiber length on pulse-distribution curves. The total concentration of pulp was 0.06 gm. per 100 ml. and the shear rate was 16 sec^{-1}*

Sample	*% Fines*	*% 48/100-mesh*	σ/N_0
1	*100*	*0*	*0.540*
2	*80*	*20*	*0.815*
3	*60*	*40*	*1.00*
4	*40*	*60*	*1.18*
5	*20*	*80*	*2.54*

Additives

From a practical point of view it was of interest to examine the effect of various chemical additives on the flocculation of pulp fibers. Additions of the following substances were studied.

(*a*) Thorium chloride,
(*b*) Aluminum sulphate,
(*c*) Deacetylated Karaya gum,
(*d*) Methyl cellulose (Dow Methocel).

Thorium chloride was investigated because it is effective in reducing and reversing the zeta-potential at the cellulose–water interface. Thus, if flocculation of fibers is analogous to coagulation of sols, variation of this quantity might alter the degree of flocculation. The remainder of the substances have been reported to decrease pulp flocculation (2, 5, 16).

The results obtained by additions of varying amounts of these substances to pulp-fines suspensions of approximately 0.07 gm. per 100 ml. concentration are shown in Table III. The effects noted in most cases are small compared with the variations resulting from varied shear and fiber length.

An exception to the small variations noted is found in the results obtained from the addition of deacetylated Karaya gum in excess. The series provides a useful illustration of the method by virtue of the wide range of flocculation

TABLE III

EFFECT OF VARIOUS ADDITIVES ON THE FLOCCULATION INDEX

Additive	Concentration,* %	Flocculation index
1. Aluminum sulphate	0	0.75
	0.4	0.78
	1.2	0.75
	2.4	0.70
	4.0	0.59
2. Methyl cellulose	0	0.76
	0.4	0.70
	1.2	0.67
	2.4	0.55
	3.6	0.64
	8.0	0.65
3. Thorium chloride	0	0.72
	0.36	0.72
	1.4	0.72
	2.9	0.72
	5.8	0.72
4 Deacetylated Karaya gum	0	0.62
	12	0.71
	30	1.72
	45	2.70
	60	3.07
	120	0.86

* *Concentration of additives are calculated relative to the oven-dry weight of pulp fibers.*

indices found. The distribution curves found are shown in Fig. 14. The experiments are uncontrolled in the sense that Karaya gum suspensions vary in effectiveness with each preparation. This experiment also emphasizes the danger of extrapolating the findings for pulp fines to suspensions of long fibers. Fig. 15 shows that, with a long-fibered stock, a comparable concentration of Karaya gum has an appreciable dispersing action.

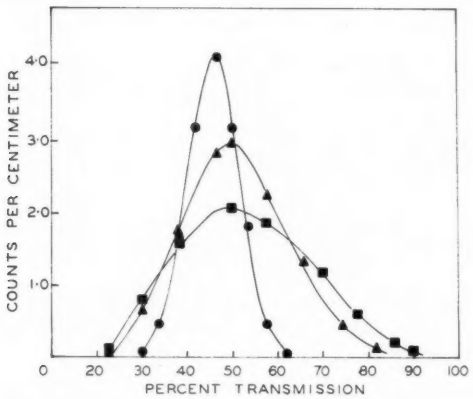

FIG. 14. *The effect of deacetylated Karaya gum on pulp fines suspensions. The concentration of pulp was 0.089 gm. per 100 ml. and the shear rate was 16 sec.*$^{-1}$ *Karaya gum concentrations were 0 (●), 0.025 (▲), 0.050 (■) gm. per 100 ml. The flocculation indices are 0.411, 1.17, and 2.06 respectively.*

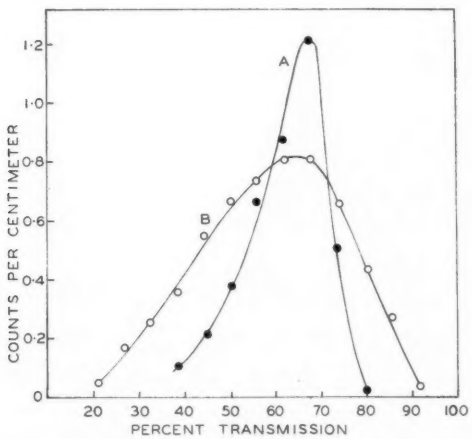

FIG. 15. *The effect of deacetylated Karaya gum on the flocculation of long fibers. The concentration of pulp was 0.052 gm. per 100 ml. and the shear rate 27 sec.*$^{-1}$ *The flocculation indices with (A) and without (B) Karaya gum are 1.15 and 5.98 respectively.*

The average photocell current was measured during each experiment. In most cases its value was found to correspond approximately to the transmission level at which the maximum counting rate was observed, but it was not sufficiently sensitive nor reliable to be used as a flocculation index. It may be seen in Figs. 10, 14, and 15 that a change in flocculation does not always produce a significant shift in the mean transmission level. This effect may be due in part to drift in the discriminator characteristics.

Discussion

The experiments described must be considered no more than exploratory in nature but they serve to demonstrate that the principle of the experimental methods is sound. The distribution curves obtained by pulse-counting and time-integration were found to have approximately the form predicted. The pulse-counting method was used in the bulk of the work since it provided an N_0 value which the other did not. The measurement of the average current proved to be more useful as a control reading than as a flocculation index.

The results also tend to confirm the prediction made concerning the effect of shear on the dynamic floc-particle equilibrium of suspensions. Furthermore the data provide some preliminary information concerning the effect of specific additives on flocculating tendency in the particular case of pulp "fines".

It must be pointed out that in the experiments concerned with additives or change in fiber length, the results must be interpreted with caution. Variation in the amount of particle–liquid surface or in the relative refractive indices of the two phases will affect the light-scattering properties of the suspensions.

The suspensions of pulp used in the experiments are well suited for this study. As a result of their weak interparticle attractive forces, the flocculation index σ/N_0 is sensitive to changes in the rate of shear. With other types of suspension the pattern of results is changed. Whole-pulp fibers form large stable flocs presumably because of increased mechanical entanglement (12), and their free growth is restricted by the dimensions of the present apparatus. For these reasons results are somewhat less reproducible than for fines, and high rates of shear (greater than 50 sec.$^{-1}$) are required to break up the flocs appreciably. Suspensions of aged latex particles in water showed very little tendency to flocculate or deflocculate at shear rates between 10 and 30 sec.$^{-1}$ and the pulse distribution remained constant in this range. Other systems such as coarse emulsions, coagulated milk, and insoluble powders could not be studied by this method because of rapid sedimentation or slowness in attaining a particle–floc equilibrium.

Certain anomalies appeared during the experimental work which impose limitations on the application of the technique in the apparatus described here.

As the shear rate is increased, the system becomes more dispersed. At sufficiently high rates of shear this action may result in the maximum counting rate

leveling off or actually decreasing, presumably because the limit of resolution of the discriminator-counting system is exceeded by the simultaneous increase in pulse frequency and decrease in pulse height.

It was noticed that as the concentration of the suspension was increased, N_0 and σ passed through a maximum. This was to be expected. As the concentration is increased, the number and size of flocs increase until the individual aggregates lose their identity owing to the increased probability of other flocs being scanned at the same time.

The design of the apparatus imposes several other limitations on the application of the method. A simple shear field is required so that scanning rate is known. The rate of shear, therefore, must be such that flow is viscous and not turbulent, and that centrifuging does not occur. The effect of the circulation of suspension on the shear field in the apparatus must be negligible. Pulp suspensions show an appreciable thixotropy in concentrations as low as 0.1%, and plug flow can be demonstrated when the concentration is sufficient to form a connected structure. Concentrations must be such that these effects are absent. Finally, the free growth of aggregates must not be hindered by the dimensions of the apparatus.

Acknowledgment

The authors are indebted to Mr. J. T. M. Taylor for assistance in the design and development of some of the electronic equipment.

References

1. BLOOMQUIST, C. R. and SHUTT, R. S. Ind. Eng. Chem. 32: 827. 1940.
2. BROADBENT, F. D. and HARRISON, H. A. Proc. Tech. Sect., Paper Makers' Assoc. Gt. Brit. & Ireland, 21: 213. 1940.
3. DAVIS, M. N., ROEHR, W. W., and MALMSTROM, H. E. Tech. Assoc. Papers, 18: 386. 1935.
4. DONALD, M. B. Chemistry and Industry, 59: 105. 1940.
5. ERSPAMER, A. Tech. Assoc. Papers, 23: 132. 1940.
6. FAVIS, D. V. and MASON, S. G. Unpublished data.
7. GALLAY, W. and PUDDINGTON, I. E. Can. J. Research, B, 21: 171. 1943.
8. GOETZ, A., GOULD, W. O., and DEMBER, A. J. Soc. Motion Picture Engrs. 34: 279. 1940.
9. GOODEVE, C. F. Trans. Faraday Soc. 35: 342. 1939.
10. KRUYT, H. R. and VAN SELMS, F. G. Rec. Trav. Chim. 62: 408, 415. 1943.
11. MASON, S. G. Pulp & Paper Mag. Can. 49 (No. 13): 99. 1948.
12. MASON, S. G. Pulp & Paper Mag. Can. 51 (No. 5): 93. 1950.
13. RICE, S. O. Bell System Tech. J. 23: 282. 1944.
14. RICE, S. O. Bell System Tech. J. 24: 46. 1945.
15. STEINOUR, H. H. Ind. Eng. Chem. 36: 618, 840, 901. 1940.
16. WOLLWAGE, J. C. Tech. Assoc. Papers, 22: 578. 1939.

VOLUMETRIC DETERMINATION OF SMALL AMOUNTS OF IRIDIUM[1]

By W. A. E. McBryde and M. L. Cluett

Abstract

A volumetric procedure is described for determining small amounts of iridium (from 2 to 20 mgm.). A solution of the metal is heated to dense fumes with sulphuric acid, cooled, diluted with water, and then oxidized with an excess of cerium (IV) sulphate solution. The resultant solution is titrated with a standard 0.01 *N* iron (II) sulphate solution, the course of the titration being followed potentiometrically. In solutions containing other platinum metals it has been found possible to determine iridium directly in some cases by this procedure; in other cases it was found necessary to remove osmium as the volatile tetroxide prior to oxidizing with cerium (IV) sulphate. The method is probably less accurate than existing gravimetric procedures, but offers considerable advantage in simplicity.

Introduction

In the course of an investigation in progress in this laboratory, a method was required for analyzing for iridium and rhodium when present together in a solution. The separation and gravimetric determination proposed by Gilchrist and Wichers (3) presented considerable difficulty because of the presence in the solutions to be analyzed of large amounts of dissolved silicates. Because a large number of analyses were contemplated, a shorter and simpler volumetric procedure was sought for this purpose. The microprocedure of Pollard (7) for iridium might have been adapted to larger samples, but, as it required a separation of rhodium from iridium and a second separation of iridium from titanium prior to the actual titration, it appeared rather time-consuming. The procedure for the determination of rhodium using thionalide, described by Kienitz and Rombock (5), was not applicable without modification because of the precipitation of iridium by that reagent. The volumetric method for rhodium proposed by Syrokomskii and Proshenkova (9) was reported in Chemical Abstracts not to be interfered with by iridium. Actually the effect of iridium upon the determination of rhodium appears not to have been investigated or reported by these authors. A few experiments have shown that the determination of rhodium is considerably affected by the presence of iridium.

In this procedure rhodium and iridium are oxidized in a sulphuric acid solution containing rhodium (III) and iridium (III) by sodium bismuthate. After removal of the residue from the latter the oxidized metal is determined by titration with standard iron (II) solution. Under the conditions recommended, rhodium is oxidized to the quinquevalent state but the oxidation of iridium proceeds to an indefinite extent, said by Syrokomskii and Proshenkova to be about 90% of a 2-electron oxidation. When this procedure was attempted with solutions containing rhodium and iridium together the titration indicated

[1] *Manuscript received July 25, 1950.*
Contribution from the Department of Chemistry, University of Toronto, Toronto, Ont.

a smaller quantity of rhodium than the amount originally introduced. Apparently when iridium is present the oxidation of rhodium is not complete. A conspicuous feature of the oxidation by sodium bismuthate in the presence of iridium is the rapid reduction of the former, shown by the evolution of gas bubbles and the conversion to the white sulphate. Furthermore, continued addition of sodium bismuthate seems only to result in its rapid decomposition. It is likely that this decomposition destroyed the excess of bismuthate required for the gradual oxidation of rhodium so that this process was incomplete.

While investigating this volumetric procedure it was found that if cerium (IV) sulphate was used in place of sodium bismuthate as oxidizing agent, iridium but not rhodium was oxidized, and it was possible to develop a volumetric method for the determination of iridium which is unaffected by the presence of rhodium.

Apparatus and Solutions

Oxidizing reagent:—A 0.1 *N* cerium (IV) sulphate solution in 0.5 *N* sulphuric acid. A sulphatocerate solution was prepared from pure ammonium cerium (IV) nitrate according to the method of Smith (8).

Reducing reagents:—Approximately 0.01 *N* iron (II) solution in 0.2 *N* sulphuric acid was prepared by dissolving the appropriate weight of ammonium iron (II) sulphate in air-free water and then diluting to the desired volume. The solution was standardized potentiometrically against a 0.01000 *N* solution of dichromate prepared from recrystallized potassium dichromate.

Approximately 0.01 *N* titanium (III) chloride solution was prepared by diluting an appropriate volume of prepared 20% titanium chloride solution (Eimer and Amend) with air-free water and diluting to a known volume. The solution was standardized similarly to the iron (II) solution.

Standard rhodium solution:—A solution of rhodium (III) chloride in 0.05 *N* hydrochloric acid was prepared so as to contain approximately 2 mgm. of rhodium per ml., and was standardized by precipitation with thiobarbituric acid (2).

Standard iridium solution:—A solution of iridium (IV) chloride in 0.05 *N* hydrochloric acid was prepared so as to contain approximately 2 mgm. of iridium per ml. and was standardized by precipitation as the hydrated oxide (4).

Standard solutions of platinum, palladium, osmium, and ruthenium:—Solutions of these metals in hydrochloric acid containing approximately 1 mgm. of metal per ml. or other known proportions were kindly provided by Prof. F. E. Beamish. These solutions were used without further standardization.

Apparatus:—Standard iron (II) and titanium (III) solutions were kept out of contact with oxygen in an apparatus such as that described by Vogel (10, page 235). A double trap of pyrogallol solution kept the air in contact with the

solution oxygen-free. A Machlette type auto burette, when equipped with pyrogallol traps, was also found to be very convenient to use with these solutions.

The potentiometric titrations were carried out with a Leeds and Northrup student potentiometer and indicating galvanometer. Some of the earlier determinations utilized a pH electrometer.

A platinum wire was used as the indicator electrode, and a saturated calomel as the reference electrode. Connection from the latter to the cell was made through an ammonium sulphate – agar salt bridge. A sintered glass disk closed the end dipping into the titration vessel. This arrangement sought to prevent contamination of the cell with chloride ion and of the calomel electrode with sulphate ion.

Experimental

A measured volume of iridium solution was diluted to about 50 ml. with water. (It was found subsequently that this dilution with water could be omitted for iridium solutions, but the determinations reported included this step.) To this was added 15 to 20 ml. of concentrated sulphuric acid. The solution was heated to eliminate water and until copious fumes were evolved by the acid; the fuming was continued for 20 to 30 min. The end of the reaction was indicated by the conversion of the brown $IrCl_6^{--}$ to the colorless sulphate. The solution was cooled and then diluted by pouring into 100 ml. of water. Excess cerium (IV) solution (usually 1 or 2 ml. of 0.1 *N*) was added to oxidize the iridium, and the solution was placed on a steam bath for at least 10 hr. The solution was then cooled to room temperature and titrated potentiometrically with the standard iron (II) or titanium (III) solution.

The oxidized iridium solution is raspberry-red in color but will show various shades depending on the amount of excess cerium (IV) present.

A typical titration curve in differential form for an iridium solution is shown schematically in Fig. 1. Tenth milliliter increments were added during the titration. Peak A represents the "end point" for the titration of excess cerium (IV). The subsequent titration of the iridium itself gives two end points as shown; the titer from A to the peak B representing a 1-electron reduction and the titer from B to the peak C representing a $\frac{1}{2}$-electron reduction. The total titer represents a $1\frac{1}{2}$-electron reduction, so that 1 mgm. of iridium is equal to 0.0078 m.e. The colored iridium solution changes to colorless shortly before the end point C is reached, providing ample warning of the approach of the end of the titration.

The total volume of iron (II) solution used in this titration (to peak C, Fig. 1) corresponded to very much less than the number of equivalents of cerium (IV) added to the solution. A blank determination containing no iridium gave a titration equivalent to the amount of oxidizing reagent added.

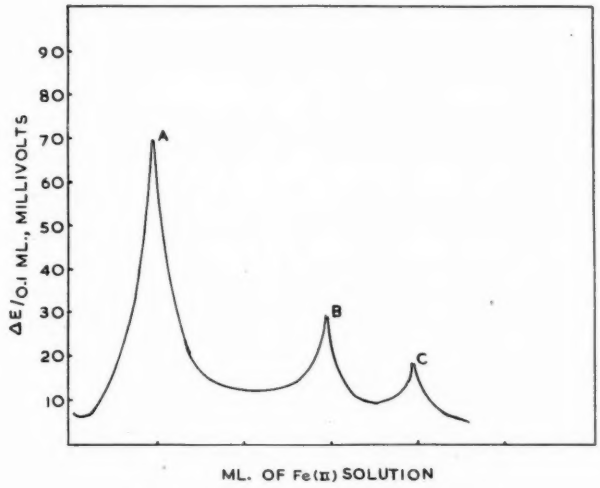

FIG. 1. *Typical titration curve for iridium.*

These observations could not be explained by the formation of any reasonable derivative of iridium. Evidently iridium catalyzed the reduction of cerium (IV) in solution under the conditions of the experiment, as shown in the following way. The procedure was followed as above with 150 μgm. of iridium and 0.2 m.e. of cerium (IV). After the heating period and cooling, titration of the solution showed a loss of cerium (IV) equal to approximately 0.14 m.e. These data are summarized in Table I. In spite of this consumption of cerium (IV) by iridium, all of the excess of the former present was not used up. Further investigation, however, revealed no quantitative relationship between the amount of iridium present and the amount of cerium (IV) consumed.

TABLE I

EFFECT OF IRIDIUM ON REDUCTION OF CERIUM (IV) ON HEATING

Amount of Ce (IV) taken, m.e.	Amount of iridium taken, m.e.	Amount of Ce (IV) titrated, m.e.
0.2	Nil	0.2
0.2	0.0012	0.058

Solutions of iridium prepared in the manner described were found to have retained, after periods as great as six weeks, an excess of cerium (IV) and to yield the same titration for iridium as those freshly prepared.

Individual solutions of each of the other platinum metals were treated in the same manner to determine any effect of cerium (IV) on them. Upon titration of each of the solutions only one end point was observed, corresponding to the reduction of the cerium (IV). However, although the amount of oxidant

added to each solution was the same, the titers of the solutions on reduction varied quite considerably. In the case of palladium there was no striking visible change and the titer for cerium (IV) was nearly equivalent to the amount added. Platinum gave some precipitate in fuming sulphuric acid which did not dissolve on dilution, and there was a noticeable loss of cerium (IV). The solutions of ruthenium turned to a rose or dark brown color on fuming with sulphuric acid, the color depending on the amount of ruthenium. As these solutions were heated with cerium (IV) this color disappeared when 2 mgm. of ruthenium was present and partially disappeared when larger amounts were taken; at the same time a black condensate appeared on the walls of the beaker and on its cover glass. On titrating the solution it was found that the greater part or all of the cerium (IV) had been reduced. Apparently the ruthenium was oxidized by these conditions to the volatile tetroxide which subsequently condensed to a lower oxide. The addition of a larger amount of cerium (IV) sulphate solution (10 ml. of 0.1 *N*) was then found sufficient to remove completely as much as 10 mgm. of ruthenium during 10 hr. on the steam bath. In the case of osmium it was found that a greenish-brown solution remained after fuming for 30 to 40 min. with sulphuric acid, and when this solution was oxidized in the prescribed manner very large amounts of cerium (IV) were reduced. Finally rhodium, the metal of particular interest in this investigation, revealed no effect on the oxidant. The titer of cerium (IV) obtained on titration was exactly equivalent to the amount added. Rhodium sulphate solution is yellow in color, and when iridium is present this color remains after the iridium is completely reduced by the titration.

In Table II are given results showing the determination of iridium in the presence of various other platinum metals. Since the immediate purpose of this research was to determine iridium in the presence of moderate amounts of rhodium, somewhat more data are available for solutions of these two metals. In the cases where platinum or ruthenium was present with the iridium the solutions were filtered before adding cerium (IV) for oxidation. For solutions containing more than 5 mgm. of osmium the procedure was modified as noted to eliminate osmium by volatilization of the oxide by adding 15 ml. of concentrated nitric acid along with the sulphuric acid and evaporating down to fumes. In a few cases the purple color due to iridium (4) persisted in these solutions, but it was possible to eliminate this by adding 10 ml. of water and again evaporating to fumes. If osmium was not completely removed prior to oxidation with cerium (IV) or if ruthenium was not completely removed during the oxidation the course of the iridium oxidation was modified in some way so that incorrect results were obtained in the titration of known samples.

Perchloric Acid Variation

Perchloric acid (72%) was used instead of concentrated sulphuric acid in the recommended procedure for determining iridium. However, no consistent titer could be obtained for a constant amount of iridium taken. Titrations ranged

TABLE II

EFFECT OF OTHER PLATINUM METALS ON THE TITRATION OF IRIDIUM

Iridium taken, mgm.	Also added	Apparent iridium recovered, mgm.
1.81	1 mgm. each of osmium, ruthenium, platinum, palladium, rhodium	1.88
3.62		3.64
5.43		5.52
7.24		7.20
9.05		9.05
3.62	10 mgm. Pt	3.66
3.62	10 mgm. Pd	3.61
3.62	14.1 mgm. Os	3.58*
3.62	7.0 mgm. Os	3.47*
3.62	7.0 mgm. Os	3.66*
3.62	7.0 mgm. Os	3.47
3.62	5.0 mgm. Os	3.69
3.62	10 mgm. Ru	3.63*
3.62	10 mgm. Ru	3.64
3.62	4.0 mgm. Rh	3.64
3.62	8.0 mgm. Rh	3.50
3.62	10.0 mgm. Rh	3.66
3.62	20.0 mgm. Rh	3.56
3.62	30.0 mgm. Rh	3.59

* *Fumed with 15 ml. nitric acid also.*

from a 1- to almost a 2-electron reduction. The titration curves showed only a single stage of reduction for the iridium. The equivalence potential for the first end point was consistently less positive than that observed for the corresponding end point in sulphuric acid solutions. This observation is unexpected in view of the fact that the standard potential for Ce (IV)/Ce (III) is known to be more positive in perchloric acid solutions than in sulphuric acid (8). These observations, which were not examined further, must be interpreted to mean that in this medium the iridium is oxidized to some other condition than that obtained in sulphuric acid. It should be pointed out, however, that the equivalence potentials for the *complete* reduction of iridium were practically identical in perchloric and sulphuric acid media.

Syrokomskii and Proshenkova (9) stated that an oxidation state of +5 would be obtained for iridium heated in perchloric acid to 207°C. They further stated that reduction of this iridium would be the basis of a volumetric determination subsequently to be described. Attempts by the present authors to reproduce these results disclosed a considerable variation in the extent of oxidation of iridium and suggested that varying amounts of oxides of chlorine remained in solution prior to titration. When these titrations were examined with the potentiometer a sharp drop in potential of the platinum electrode occurred when a fraction of a milliliter of iron (II) solution had been added. Subsequently a less definite end point accompanied by disappearance of color indicated the reduction of iridium. The first drop in potential was interpreted to be the reduction of products of decomposition of perchloric acid.

Titanium (III) Variation

To establish whether or not the two end point reduction of the iridium was peculiar only to the iron (II) reagent, a standard titanium (III) solution was prepared to use in several reduction titrations. The results showed no differences from the iron (II) titrations.

Effect of Temperature

The dependence of the rate of oxidation on temperature is shown in Table III. It was quite difficult to determine for sure the minimum time for complete oxidation of iridium since the process is fairly slow. From a number of determinations it was found that complete oxidation could be assumed after the solution had stood on the steam bath for 10 hr. Most of the results given in this report were obtained from solutions which were oxidized overnight.

TABLE III

EFFECT OF TEMPERATURE ON OXIDATION OF IRIDIUM BY CERIUM (IV)
Iridium taken = 3.62 mgm.

	Hot oxidation	Room temperature oxidation
Ml. of 0.01 *N* Fe (II) solution used to titrate iridium	2.83 2.78 2.75 2.80	2.25 2.30 2.51 2.07

A direct oxidation titration of the iridium was attempted using a standard cerium (IV) solution, but was found to be impossible. Although the iridium (III) solution was kept steaming hot the oxidation process appeared to be too slow for a potentiometric titration.

Table IV indicates that temperature has no noticeable effect on the reduction titration.

TABLE IV

EFFECT OF TEMPERATURE ON REDUCTION TITRATION OF IRIDIUM

	Iridium taken =	3.62 mgm.	7.24 mgm.
Ml. of 0.01 *N* Fe (II) solution required	Titrated hot " cold (7°C.) " 25°C.	2.84 2.90 2.81	5.68 5.48 5.62

Discussion of Results

Table V includes the results of a number of representative determinations in order to indicate what accuracy and precision may be expected from this procedure as an analytical method for iridium. It will be seen that the relative error in these determinations is greatest for the smallest samples. This is to be expected, first because the volume of reducing solution is small, and, second

TABLE V

ACCURACY AND PRECISION OF THE METHOD

Mgm. of iridium taken	Mgm. of iridium determined	% error
1.81	1.76	− 3.8
1.81	1.85	2.2
1.81	1.83	1.1
1.81	1.73	− 4.4
1.81	1.58	−12.7
3.62	3.68	1.6
3.62	3.67	1.4
3.62	3.60	− 0.6
7.24	7.30	0.8
10.86	10.77	− 0.5
18.10	18.18	0.4

because this volume is obtained as a difference between two "end points" each of which requires the interpretation of changes in potential of the indicator electrode. Probably the average error for samples of 5 mgm. or greater will be within 1%. The authors were desirous of establishing the validity of the method for small quantities of iridium and have included numerous results for samples containing less than 5 mgm. of iridium.

In Table VI are given the data from a representative titration, showing the potentials of the indicator electrode (vs. S. C. E.) near the equivalence points and the mode of interpreting these. The difference between the first and final end points has been used in calculating amounts of iridium titrated. The individual values for the equivalence points were obtained by calculating from the second differences as tabulated (6).

TABLE VI

REPRESENTATIVE DATA FOR TITRATION OF 3.62 MGM. OF IRIDIUM WITH STANDARD FE (II) SOLUTION

E.m.f. measured vs. S.C.E.

Burette readings, ml.	E	First difference	Second difference	Calculated end point
1.80	1.0733			First end point
		243		
1.90	1.0490		+377	$1.90 + 0.1 \times \frac{377}{412}$
		620		
2.00	0.9870		− 35	$= 1.99$ ml.
		585		
2.10	0.9285			
		314		
2.20	0.8971			
....	.....	...	.....	.....
3.80	0.7487			Intermediate end point
		207		
3.90	0.7280		+ 70	$3.90 + 0.1 \times \frac{70}{204}$
		277		
4.00	0.7003		−134	$= 3.93$ ml.
		143		
4.10	0.6860			
		115		
4.20	0.6745			
....	.....	...	.....	.....
4.60	0.6419			Final end point
		169		
4.70	0.6250		+256	$4.70 + 0.1 \times \frac{256}{401}$
		425		
4.80	0.5825		−145	$= 4.77$ ml.
		280		
4.90	0.5545			
		104		
5.00	0.5441			

Attempts were made to oxidize iridium in the form $IrCl_6^{--}$ with cerium (IV). Titration with standard iron (II) solution showed that all the cerium (IV) added was consumed and a titer equivalent to a 1-electron reduction was obtained for the iridium. However it had been previously shown that the original $IrCl_6^{--}$ solution on titration showed the same 1-electron reduction. The consumption of cerium (IV) in the previous case was explained by the oxidation of chloride ions to chlorine. This was verified by running a blank with dilute hydrochloric acid and cerium (IV) solution. The yellow color of the latter quickly disappeared when the solution was warmed on a steam bath for several minutes.

When a solution of $IrCl_6^{--}$ was heated to fuming with sulphuric acid and then titrated with standard iron (II) solution, no reduction took place and the potential of the indicator electrode at once assumed a value corresponding to the Fe (III)/Fe (II) system. This was taken to indicate that mild fuming with sulphuric acid reduces iridium to the +3 state. This necessitates postulating a net oxidation state of $+4\frac{1}{2}$ for iridium after oxidation with cerium (IV).

Color of the Iridium Solution

Solutions of the oxidized iridium were prepared containing known amounts of the metal and examined for absorption of monochromatic light in the visible region. One solution was titrated with iron (II) to the first equivalence point to remove excess cerium (IV), and another was titrated to the intermediate end point (peak B) for iridium. Measurements of the extinction at intervals of 10 mμ, made with a Beckman Model D spectrophotometer, resulted in the curves shown in Fig. 2. Solutions of the apparent $+3\frac{1}{2}$ oxidation state are represented by the broken curves, and solutions of the fully oxidized iridium are represented by the solid curves.

These curves may be interpreted to mean that the two solutions contain different absorbing species. It is seen that there is a noticeable difference in the wave length of the extinction maxima, and the curves would yield different values for the specific extinction of the two solutions which contain the same amount of iridium. It is interesting to compare the absorption curves of these solutions with those obtained by Ayres and Quick (1) for solutions resulting from heating iridium with mixed perchloric and phosphoric acids. The purple color obtained by these authors is probably that described by Pollard (7) and by Hill and Beamish (4); it can be shown that an almost identical extinction curve results from the oxidation of iridium by periodic acid with hot sulphuric acid.

The color of the iridium solution obtained in this investigation appeared to change on standing. The extinction curves after 7 and 12 days show that the extinction for the $+3\frac{1}{2}$ solution changes moderately while that of the $+4\frac{1}{2}$ solution undergoes relatively little change. Portions of these solutions containing known amounts of iridium were titrated at the end of this time and the observed titers showed no change in the oxidation states. It has been

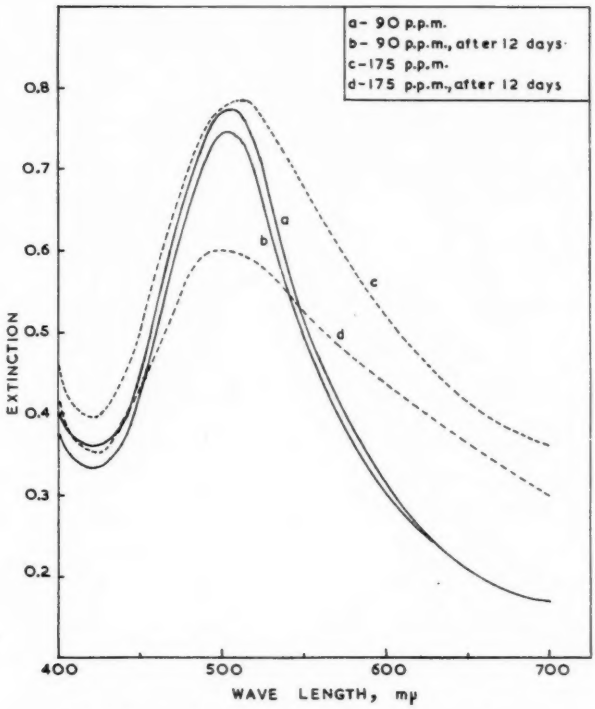

FIG. 2. *Spectrophotometric extinction for iridium solutions.*
Solid curve—oxidation state 4½.
Broken curve—oxidation state 3½.

mentioned above that the color in these solutions disappears outright somewhere between the two equivalence points B and C. This evidence suggests that there may be no direct connection between the color of the solutions and the oxidation states of the iridium.

The results obtained by Syrokomskii and Proshenkova (9) and those described in this paper require the assumption of uncommon oxidation states for iridium. Ayres and Quick (1) described the potentiometric titration of the iridium solution in mixed acids by which they sought to establish that the oxidation state of iridium in this medium was +4. Their procedure was repeated in this laboratory, and on several samples of varying amounts of iridium the titer was about 10% higher than that required for a 1-electron reduction. Pollard (7) also recorded that the titer observed when iridium, previously oxidized by perchloric acid, was reduced by standard hydroquinone solution was consistently higher than that required for a 1-electron reduction. These observations suggest no ready explanation of the structural changes accompanying these oxidations and reductions. Oxidation states of $4\frac{1}{2}$ or $3\frac{1}{2}$ presumably

indicate the formation of an ion or molecule containing two kinds of iridium atoms, but give no clue to the mode of their grouping.

The oxidized iridium solution yielded no solid derivative containing iridium when treated with various water-soluble organic liquids or with moderately concentrated solutions of salts of magnesium, zinc, silver, copper (II), nickel, iron (III), mercury (II), or lithium. The addition of alkali produced a black flocculent precipitate like that of a hydrous oxide in appearance. This was found to be of no value in identification because of the presence of considerable oxides of cerium. Some effort will be made to precipitate these oxides at controlled pH, in the hope of producing a sample of the iridium derivative in a state of purity sufficient for X-ray and other examination. Unfortunately, even evidence of the structure of the oxide derived from the oxidized iridium solution affords no sure evidence of the nature of the colored constituent in solution. With the present limited information the procedure described gives only an empirical method for the analytical determination of iridium. However, this method offers advantages in speed and simplicity, owing especially to the fact that no procedure for the elaborate separation of the other platinum metals is required.

References

1. AYRES, G. H. and QUICK, Q. Anal. Chem. 22: 1403. 1950.
2. CURRAH, J. E., MCBRYDE, W. A. E., CRUIKSHANK, A. J., and BEAMISH, F. E. Ind. Eng. Chem., Anal. Ed. 18: 120. 1946.
3. GILCHRIST, R. and WICHERS, E. J. Am. Chem. Soc. 57: 2565. 1935.
4. HILL, M. A. and BEAMISH, F. E. Anal. Chem. 22: 590. 1950.
5. KIENITZ, H. and ROMBOCK, L. Z. Z. Anal. Chem. 117: 241. 1939.
6. KOLTHOFF, I. M. and FURMAN, N. H. Potentiometric titrations. 2nd ed. John Wiley and Sons, Inc., New York. 1931.
7. POLLARD, W. B. Bull. Inst. Mining Met. 497: 9. 1948.
8. SMITH, G. F. Cerate oxidimetry. The G. Frederick Smith Chemical Co., Columbus, Ohio. 1942.
9. SYROKOMSKII, V. S. and PROSHENKOVA, N. N. Zhur. Anal. Khim. 2: 247. 1947. Chem. Abstracts, 43: 5698. 1949.
10. VOGEL, A. I. Quantitative inorganic analysis. Longmans Green and Co., London. 1939.

THE OXIDATION OF CARBON MONOXIDE BY SOLID SILVER PERMANGANATE REAGENTS

II. KINETIC STUDIES WITH SILVER PERMANGANATE – ZINC OXIDE[1]

By Morris Katz, G. A. Grant, and R. Riberdy

Abstract

The kinetic equations of the adsorption wave were applied to the oxidation of carbon monoxide in an air stream by granular silver permanganate – zinc oxide reagent. The following relations have been investigated in this system: (*a*) the concentration of the escaping gas as a function of time, (*b*) the effect of initial concentration, column length, and flow rate on breakdown time, (*c*) the influence of granule size on breakdown time and rate of reaction. The critical column length was found to be dependent on flow rate and independent of initial concentration. Critical column lengths of approximately 0.4 cm. to 1 cm. were found for the range of flow rates studied. The relation found between granule size and breakdown time does not completely agree with the theoretical equations. As the mean diameters of the granules decreased from 2.2 mm. to 0.90 mm. the breakdown time increased, but a decrease in mean diameter from 0.90 to 0.30 mm. resulted in a reduction of breakdown time. Although the results are in general agreement with the equations developed by Hinshelwood and Klotz, certain deviations from the theoretical treatment were evident.

Introduction

The oxidation of carbon monoxide by silver permanganate – metallic oxide reagents was reported by Katz *et al.* (7). Of the reagents compounded, a silver permanganate–zinc oxide mixture appeared to be the most effective for oxidizing carbon monoxide in an air stream. One of the advantages of these active granules over the hopcalite type is that they are not poisoned by the water vapor in the air. In fact, optimum activity is exhibited when the air is at about 50–80% relative humidity at room temperature.

The present paper deals with the oxidation of carbon monoxide in a flowing air stream on passage through a bed of granular silver permanganate – zinc oxide. The following relations have been investigated in this system: (*a*) the concentration of the escaping gas as a function of time, (*b*) the effect of initial concentration, column length, and flow rate on breakdown time, (*c*) the influence of granule size on breakdown time and rate of reaction.

As carbon monoxide is removed completely by chemical reaction at the surface of the granules, there should be no back pressure of carbon monoxide on the reagent, and therefore the kinetics of the reaction in a flow system should closely parallel the kinetics of irreversible adsorption in a reaction bed (for example, the removal of arsine and hydrogen sulphide by impregnated charcoal).

If a sound theoretical adsorption wave expression could be applied to this problem, it would greatly reduce the number of experiments necessary to define

[1] *Manuscript received August 18, 1950.*
Contributed as Report No. 52 from Defence Research Chemical Laboratories, Ottawa, Canada. Presented at the Annual Conference of the Chemical Institute of Canada, Toronto, June 1950.

completely the geometry of the bed in relation to design of respirator canisters. Equally important would be the elucidation of the mechanism of adsorption of various gases on different types of adsorbents, from which information could be derived for their improvement or to indicate when the adsorbent has attained its maximum efficiency.

Theoretical treatment of the problem has been made by various investigators (2, 5, 10). However, these workers did not have sufficient experimental data to support their views. The problem of adsorption by charcoal was treated by Wicke (11) and a number of useful differential equations derived. However, a real advance in the solution of this problem was made only recently by a number of investigators (1, 4, 9). From a previous investigation (7) it was evident that the removal of carbon monoxide by silver permanganate reagents was controlled by a single rate-controlling step. Diffusion undoubtedly plays a role in the removal mechanism and the various steps in the process have been mentioned by Klotz (9). Whether surface reaction or diffusion (mass transfer) to the surface becomes the rate-controlling step will become evident in the analysis of the experimental data with respect to the rate constant.

General Theory

A fundamental equation, which is independent of any assumptions, can be derived by considering the mass balance in the system. The following equation or ones similar in form have been derived by many investigators (4, 10, 11).

$$-\frac{\partial x}{\partial t} = L\frac{\partial c}{\partial \lambda} + \frac{\partial c}{\partial t}, \tag{1}$$

where c = Concentration of gas in moles per unit volume in air stream,
x = Number of moles of gas removed per unit volume of bed,
V = Volume rate of flow,
A = Cross-sectional area of tube,
L = Linear flow rate, $L = \frac{V}{A}$,
t = Time of contact,
λ = Depth of bed or column length.

To obtain a solution of this equation, Danby *et al.* (4) assumed that the rate of removal of the gas from the air stream is proportional to both the concentration of active centers and the concentration of gas in the air stream. Hence $-\frac{\partial x}{\partial t} = kcN$, where k is a constant and N is the number of active centers per cubic centimeter of material. If N_0 is the number of active centers present initially, then $(N_0 - n) = N$. By substituting kcN for $-\frac{\partial x}{\partial t}$, one can simplify the equation to

$$kcN = L\frac{\partial c}{\partial \lambda} + \frac{\partial c}{\partial t}. \tag{2}$$

The following additional assumptions have been made (4):

(*a*) Active centers gradually lose their activity as the gas is removed by chemical reaction. It is assumed that on the average each active center deals with a given number of molecules of gas before becoming inactive.

(*b*) The heat of reaction or of adsorption is conducted away immediately and has no effect on the rate or the adsorbent.

(*c*) Local changes of water content do not alter the rate of removal.

A particular mathematical solution of the equation, based on the above assumptions, has been found by Amundson (1). This has the form

$$\ln(c_0/c - 1) = -kc_0T + \ln(e^{kN_0\lambda/L} - 1), \tag{3}$$

where T = total time of exposure of the reaction bed, c_0 is the initial concentration of carbon monoxide in the gas stream, c is the escaping concentration from the reagent bed, and N_0 is the number of active centers present initially. Putting $c = c^1$ and $T = \tau$, Equation (3) can be rearranged to give:

$$\tau = \frac{1}{kc_0}\left[(\ln e^{kN_0\lambda/L} - 1) - \ln(c_0/c^1 - 1)\right], \tag{4}$$

where τ is the breakdown time in minutes, c^1 = an arbitrarily chosen escaping concentration of gas from the column, and k = the rate constant. This equation may be arranged to study the effect of flow rate, column length, and initial concentration on breakdown time and hence to evaluate the critical condition for each variable.

Based on the assumptions that the number of active centers is proportional to the "accessible" area, and that accessible area attains a definite limit as the granule size is reduced, the following relation for the effect of granule size has been derived by Danby *et al.*(4).

$$N_0 = S\,(1 - \alpha d), \tag{5}$$

where S is the limiting value of N_0, when d, the mean diameter of the granules, is very small, and α is a constant.

Thus, the complete breakdown time equation now becomes

$$\tau = \frac{\lambda}{c_0L}S(1 - \alpha d) - \frac{1}{kc_0}\ln c_0/c^1 \tag{6}$$

if unity is neglected in comparison with $e^{kN_0\lambda/L}$ and $\ln c_0/c^1 >> 1$.

In view of the number of assumptions that have been made in deriving the adsorption wave equations and considering the fact that no experimental data are available for adsorption of gas in a flow system on materials other than charcoal, experimental work was carried out to evaluate the critical conditions for each variable in the equation.

Material and Experimental Methods

The reagent employed in the following experiments contained 69 mole % of zinc oxide and 31 mole % silver permanganate. The method of preparation of the reagent has already been outlined in a previous publication (7). The reagent was broken up into small granules and screened to the granule size desired, −8 to +28 Tyler, for all experiments except in the study of the effect of granule size. The granules were aged for 72 hr. at 60°C. and then stored in a brown glass bottle until required. The preparation and purification of the carbon monoxide have already been described in a previous paper (7).

The apparatus employed in these experiments has been previously described (7). The concentration of the escaping carbon monoxide was detected by means of a thermocouple cell filled with silver permanganate – zinc oxide reagent (8) and calibrated using the iodine pentoxide method (6). By employing the thermocouple cell technique, the concentration of the escaping gas could be followed almost instantaneously over the range of 0.001 to 0.1%. This was a decided advantage when high flow rates were investigated, as detectable concentrations may appear in the effluent gas within five minutes or less. The influent gas concentrations were made up by metering the air and carbon monoxide by means of calibrated flow meters. The reaction tube was immersed in a water bath maintained at 30°C. in an effort to keep the reaction bed at a uniform temperature. All conditions such as flow rate, relative humidity of air, and temperature were maintained constant as far as possible during a given experiment. The effect of flow rate and gas concentration was studied over the range of 313 to 1250 cm. min.$^{-1}$ and at concentrations of 0.25 to 1.0% carbon monoxide in a glass tube with a diameter of 2.84 cm., and column lengths of 1 to 8 cm. of reagent.

Investigation of the effect of varying the mean diameter of the granules from 0.30 to 2.20 mm. was also carried out. To measure the surface area of the granules the B.E.T. method (3) was employed.

Results

Relation Between the Concentration of Escaping Gas and Time

The breakdown time of a column has been defined as the time at which the concentration of the escaping gas exceeds an arbitrarily chosen c^1, which in the present case was 10% of the influent concentration.

Equation (3) predicts that on plotting the logarithm of the reciprocal of the concentration of the gas escaping from the column, against the time, a straight line should be obtained. A few of the results are shown in Fig. 1. For most of the cases the relation was well obeyed. However, there were deviations at very low escaping concentrations. Many of the deviations could have been caused by errors in analysis due to drift caused by small thermal effects around the cold junction of the thermocouples.

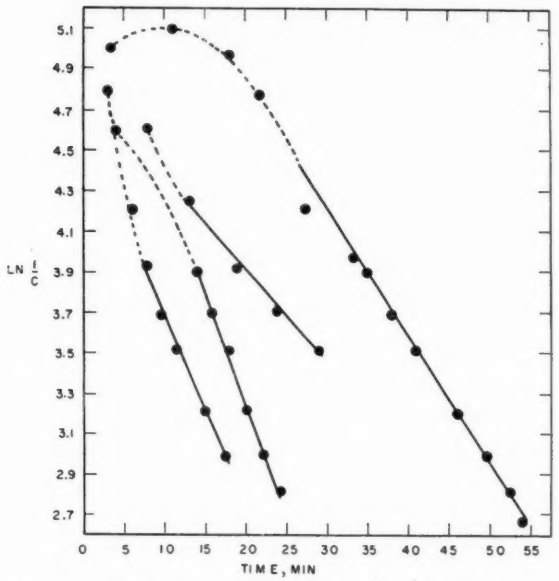

FIG. 1. *Relation between the concentration of the escaping carbon monoxide and time.*

The slope of the line taken at the higher escaping concentrations represents the value of kc_0 and hence k for each condition studied. These values were calculated for the experiments and will be discussed in a following section.

Effect of Column Length

From the equation
$$\tau = \frac{N_0}{c_0 L}(\lambda - \lambda_c), \tag{7}$$
which is obtained by substitution of λ_c, the critical column length, for λ at instantaneous breakdown, when $\tau = 0$, in Equation (4) and neglecting unity in comparison with $e^{kN_0\lambda/L}$, the breakdown time should increase linearly with column length after a critical length has been passed. It should also be inversely proportional to the concentration of the gas in the entering stream. The quantity N_0, the concentration of active centers, may be calculated from the slope of the curve. c_0 should be expressed, here, in units of molecules per cubic centimeter. From Fig. 2 it is evident that the relation is well obeyed, and the critical column lengths (Table I) vary from 0.35 cm. to 1.0, depending on the flow rate. The effect of flow rate on the critical column length will be discussed in a later section.

From the slope of the breakdown time – column length curves, the N_0 values have been calculated. The results are shown in Table II. The N_0 values vary from 2.6×10^{21} to 4.1×10^{21}. There was no pronounced effect produced on the value of N_0 by changes in flow rate or initial concentration.

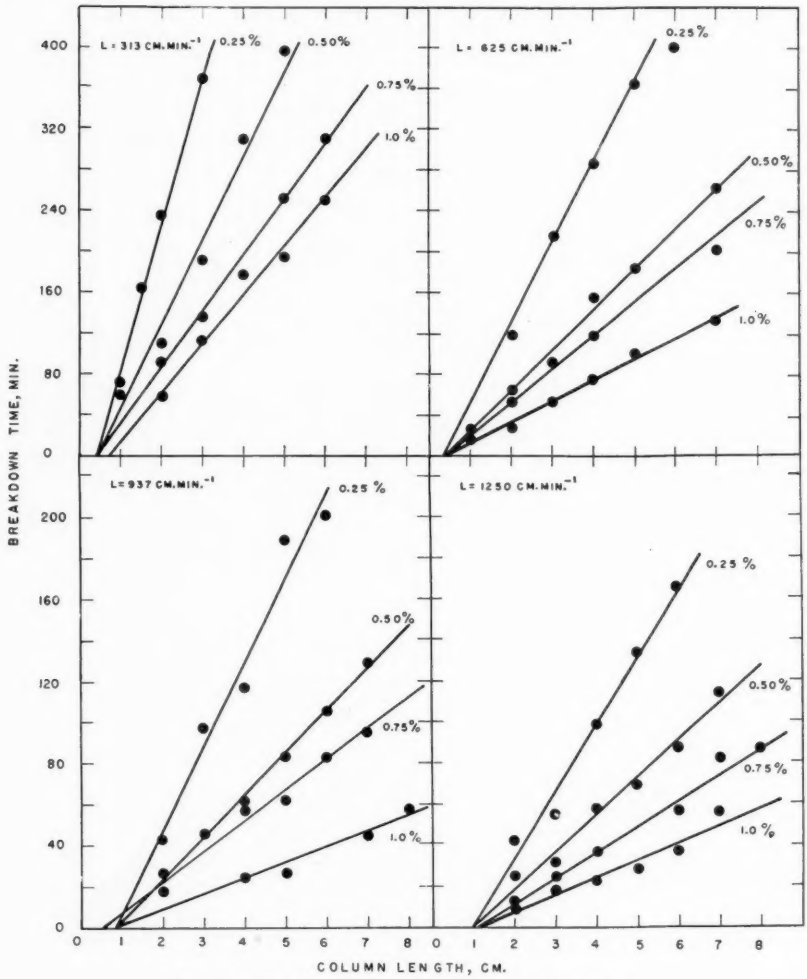

FIG. 2. *The effect of column length on breakdown time.*

TABLE I

EFFECT OF FLOW RATE AND INITIAL CONCENTRATION ON CRITICAL COLUMN LENGTH

Flow rate, cm./min.	Critical column length, cm.			
	CO 0.25%	CO 0.50%	CO 0.75%	CO 1.00%
313	0.45	0.45	0.45	0.70
625	0.35	0.35	0.35	0.35
937	0.85	0.85	0.50	0.85
1250	0.95	0.95	1.00	1.00

TABLE II

EFFECT OF FLOW RATE AND INITIAL CONCENTRATION ON N_0

Flow rate, cm./min.	N. × 10^{-21} Number of active centers per cc.			
	CO 0.25%	CO 0.50%	CO 0.75%	CO 1.00%
313	—	3.5	3.5	4.1
625	3.3	3.3	4.1	2.7
937	3.0	2.6	3.0	—
1250	2.7	3.1	3.1	2.8

Mean value, 3.2×10^{21}

Effect of Flow Rate

From the equation

$$\tau = \frac{N_0 \lambda}{c_0}\left(\frac{1}{L} - \frac{1}{L_c}\right), \tag{8}$$

which may be obtained by substituting L_c, the critical flow rate, for L, when $\tau = 0$, in Equation (4), neglecting unity in comparison with the exponential term, a linear relation should exist between the breakdown time and the reciprocal of the flow rate. c_0 is expressed in units of molecules per cubic centimeter. The intercept on the $1/L$ axis represents the critical flow rate, L_c, for which the column should break down immediately. As the flow rate and column length effects are closely related, any change in the flow rate should alter the critical column length and the slope of the column length – breakdown time curve.

The results of varying both the column length and flow rate are given in Table III. It is evident by the increase in kc_0 with flow rate, that the flow rate alters the slope of the curves as shown in Fig. 3.

TABLE III

EFFECT OF FLOW RATE AND COLUMN LENGTH ON BREAKDOWN TIME AND $kc_0/2.3$

Initial concentration, 1.0%

Column length, cm.	L – 313 cm./min.		L – 625 cm./min.		L – 937 cm./min.		L – 1250 cm./min.	
	Min.	$kc_0/2.3$	Min.	$kc_0/2.3$	Min.	$kc_0/2.3$	Min.	$kc_0/2.3$
2	60	0.048	34	0.060	9	0.10	8	0.23
3	110	0.035	54	0.056	17	0.13	16	0.23
4	159	0.035	76	0.048	25	0.13	25	0.19
5	206	0.035	96	0.048	33	0.13	36	0.12
Mean		0.038		0.053		0.12		0.19

This dependence of k, the rate constant, on flow rate indicates that the surface chemical reaction takes place more rapidly than the diffusion of carbon monoxide molecules to the solid. The latter process is therefore the rate-controlling step and the effect on rate constant will be given by $k_D = k/\mathrm{L}^n$, where k_D is proportional to the diffusion constant of carbon monoxide in air. The value of n is usually about 0.5 (4). However, substitution of this value did not give constant k_D values, as shown in Table IV. Better agreement was obtained by substituting $n = 1$.

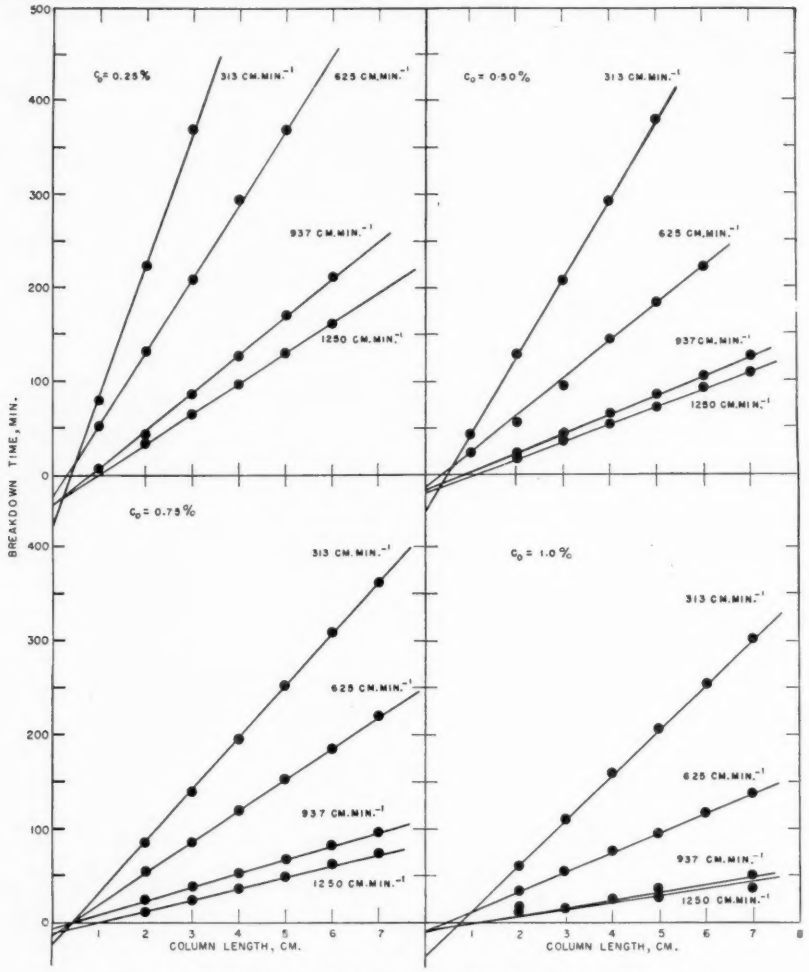

FIG. 3. *The effect of flow rate and column length on the breakdown time.*

TABLE IV

EFFECT OF FLOW RATE ON k AND λ_c VALUES
Conditions: column length, 4 cm.; initial concentration, 0.50%

L, cm./min.	K	λ_c	$d\tau/d\lambda$	$k/L^{\frac{1}{2}}$	k/L	$\lambda_c/L^{\frac{1}{2}}$	λ_c/L	$Ld\tau/d\lambda$
313	161	0.50	82.5	9.1	0.52	0.028	16.0	25,800
625	238	0.45	37.5	9.5	0.38	0.018	7.2	23,400
937	426	0.80	20.0	13.8	0.46	0.026	8.5	18,750
1250	547	1.0	18.8	15.4	0.44	0.028	8.7	23,500

Although Danby *et al.* (4) found λ_c to be dependent on $L^{\frac{1}{2}}$ in their work on charcoal, from Fig. 3 and Table IV it is evident that λ_c also shows some dependence on flow rate, as $\frac{\lambda_c}{L}$ is fairly constant at one concentration, 0.50% carbon monoxide. However, in the data from experiments on the three other concentrations, λ_c showed many irregularities, but always increased with increasing flow rate. It is also evident from the slope of the lines in Fig. 3 that $\frac{d\tau}{d\lambda}$ is inversely proportional to the flow rate.

The relation between τ and $\frac{1}{L}$ is shown in Fig. 4 and appears to be linear. Values of the critical flow rate, L_c, are given in Table V. The critical flow rates varied with column length for column lengths of 1 to 3 cm. and then remained unchanged. At short column lengths the L_c's are much higher than at column lengths of 3 cm. or greater. The initial concentration had no effect on the L_c values.

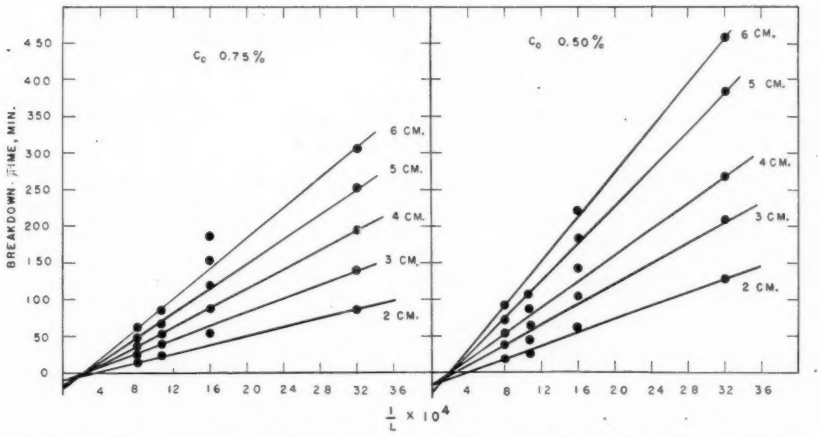

FIG. 4. *The relation between the reciprocal of the flow rate and breakdown time for different column lengths.*

TABLE V

EFFECT OF INITIAL CONCENTRATION AND COLUMN LENGTH ON THE CRITICAL FLOW RATE, L_c

c_0	$1/L \times 10^{-4}$					
	1 cm.	2 cm.	3 cm.	4 cm.	5 cm.	6 cm.
0.25%	–	4	2.8	2.2	–	–
0.50%	–	4	2.8	2.1	2.2	2.1
0.75%	8	4	3.0	2.4	2.5	2.1
1.00%	–	4	2.8	2.6	–	–

Effect of Initial Concentration

The critical concentration is given by the equation

$$c_{0_c} = c^1 \, e^{kN_0\lambda/L}, \tag{9}$$

and it can be seen from Equation (4) that a plot of τ versus $1/c_0$ should be linear and that the intercept on $1/c_0$ axis will be c_{0_c}, the critical initial concentration.

Experiments were carried out at four different initial concentrations at various flow rates. From this and previous studies (7), a linear relation was evident but the critical initial concentration varied with flow rate. The critical values appeared to be over 2% carbon monoxide for instantaneous breakdown. However, although no data are given here, it is evident from observations that initial concentrations of over 1% sometimes caused the reagent to break down into a fine powder and plug the reaction tube. When high flow rates were used these heat effects were magnified to the extent that thermal decomposition of silver permanganate was a prominent factor in the breakdown of the reagent.

Effect of Initial Concentration on Critical Column Length and Critical Flow Rate

The influence of the initial concentration has been studied over a series of flow rates. The data for experiments conducted with a linear flow rate of 625 cm. per minute are given in Table VI. The critical column length is not affected by the initial concentration. Therefore, the linear relation between λ_c and log c_0 was not confirmed. It is also evident from Table VI that the predicted inverse proportionality between $\frac{d\tau}{d\lambda}$ and c_0 is not confirmed.

TABLE VI

THE EFFECT OF INITIAL CONCENTRATION AND COLUMN LENGTH ON BREAKDOWN TIMES

Column length, cm.	Breakdown time, min.			
	c_0 0.25%	c_0 0.50%	c_0 0.75%	c_0 1.0%
2	132	26	20	12
3	210	56	54	34
4	290	95	86	54
5	368	144	120	76
6	–	184	152	96
7	–	222	185	116
8	–	262	220	138
$d\tau/d\lambda$	80	65	57	40
λ_c	0.36	0.45	0.45	0.45
$c_0 d\tau/d\lambda$	20	32.5	42.8	40

The results of the study of the variation of breakdown time with flow rate at various initial concentrations are shown in Fig. 5. The values for $1/L_c$ derived from Fig. 5 are given in Table VII. From the relation

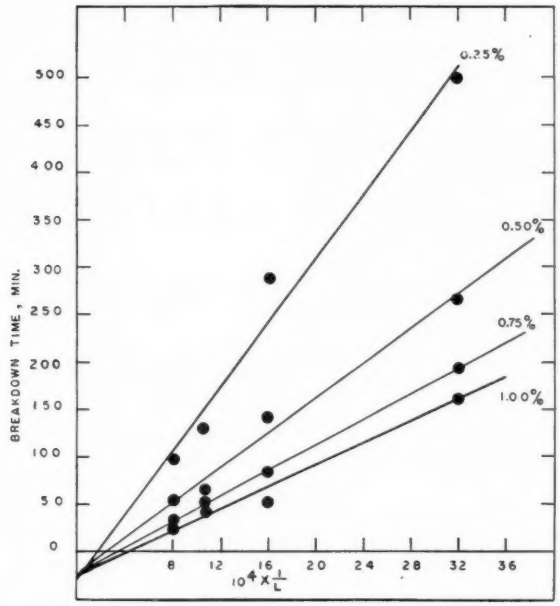

FIG. 5. *Effect of initial concentration on breakdown time and critical flow rate.*

TABLE VII

EFFECT OF INITIAL CONCENTRATION ON CRITICAL FLOW RATE

Initial, concentration, %	Critical flow rate $1/L_c \times 10^{-4}$
0.25	1.8
0.50	2.2
0.75	3.2
1.00	4.0

$$L_c = \frac{N_0 k \lambda}{\ln(c_0/c^1 - 1)} \tag{10}$$

$1/L_c$ should vary linearly with log c_0. This was not confirmed in the present case. $1/L_c$ varied linearly with c_0 (Fig. 6) but did not satisfy boundary conditions, as the curve did not pass through the origin. The critical flow rate was doubled from 2500 cm. per min. to 5100 cm. per min. for a fourfold change in concentration of 1.0 to 0.25% carbon monoxide. These flow rates appear high, as it has already been pointed out that flow rates of the order of 1250 cm. per min. are near the critical region for an initial concentration of 1.0%.

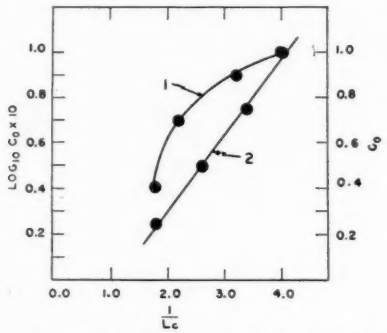

FIG. 6. *Relation between initial concentration and critical flow rate.*
(1) refers to log scale.
(2) refers to linear scale.

Effect of Granule Size

The relation

$$(\tau + \tau_0) = N_0 \frac{\lambda}{c_0 L} \tag{11}$$

can be derived from Equation (3) by putting $\tau_0 = 1/kc_0 \ln (c_0/c^1 - 1)$ and neglecting unity in comparison with the exponential term. The constant k can be found in terms of $\frac{N_0\lambda_c}{c_0 L}$ as $\ln c_0/c^1 = \frac{kN_0\lambda_c}{L}$. Equation (11) predicts that column length–breakdown time curves for various granule sizes should intersect

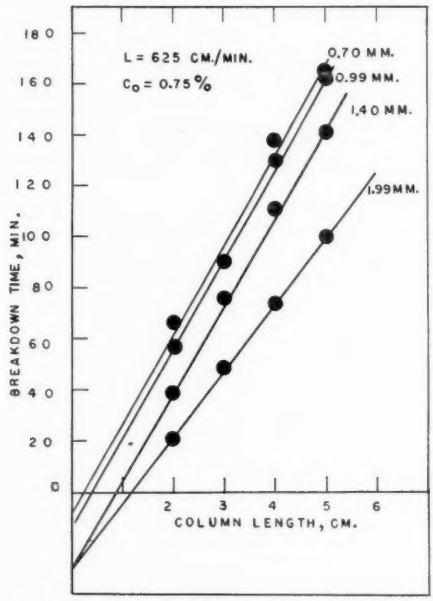

FIG. 7. *Effect of granule size and column length on breakdown time and critical column length.*

on the τ axis at $-\tau_0$. The variation of slope with granule diameter will give the relation between N_0 and granule size. The column length – breakdown time curves for four different granule sizes are shown in Fig. 7. The intercept on the τ axis at $-\tau_0$ is constant for the two larger granule sizes but differs markedly for the smaller granule sizes.

Although the equations predict that k is independent of granule size for charcoal, in the case of the silver permanganate k is dependent on granule size. A plot of $d\tau/d\lambda$ against mean granule diameter in the case of charcoal gave a straight line (4). The results with silver permanganate are shown in Fig. 8. It is evident that the relation is not linear. If linearity had existed for the plots, the expression N_0 would have been of the form, $N_0 = S(1 - ad)$. Thus the equation predicted for granule size is not confirmed. Furthermore, a plot of

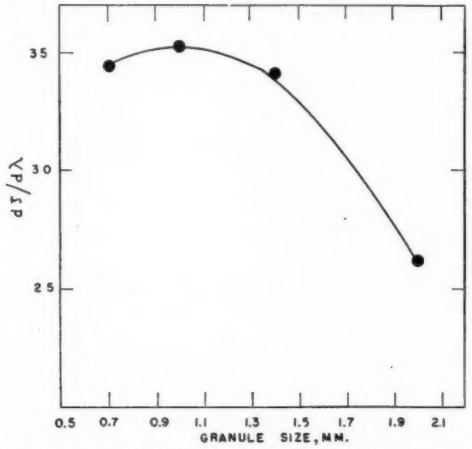

FIG. 8. *Relation between granule size and slopes of column length – breakdown time curves.*

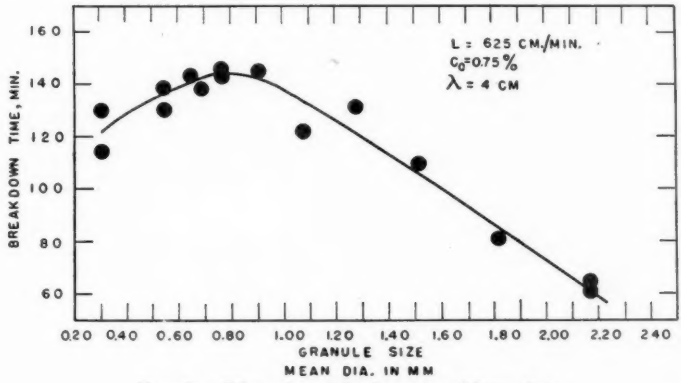

FIG. 9. *Effect of granule size on breakdown time.*

granule size with breakdown time for a number of granule sizes, as shown in Fig. 9, indicates that τ increases with decreasing granule size, goes through a maximum at 0.85 mm., and then decreases. This relation does not substantiate the functions put forth by Danby *et al.* and so the over-all Equation (6) for predicting breakdown time, cannot be applied to the gas–solid reaction for the oxidation of carbon monoxide by silver permanganate – zinc oxide.

From Table VIII it is evident that kc_0 decreases with increasing granule size, and is inversely proportional to the granule size in the range of 0.55 mm. to 1.82 mm. The assumption that breakdown time is dependent on an increase in surface area is not confirmed. In Table IX, measurements of the surface area by the B.E.T. method (3) are given for three different granule sizes. The results show that actual surface area is not greatly affected by granule size.

TABLE VIII

EFFECT OF GRANULE SIZE ON kc_0

Granule size, d, mm.	kc_0	$kc_0 \times d$
0.31	0.094	0.029
0.46	0.239	0.110
0.55	0.117	0.064
0.65	0.103	0.067
0.77	0.084	0.065
0.91	0.074	0.067
1.08	0.069	0.074
1.28	0.052	0.065
1.52	0.048	0.073
1.82	0.036	0.065
2.17	0.036	0.078

TABLE IX

EFFECT OF SURFACE AREA ON BREAKDOWN TIME

Granule size diam., mm.	Min.	Surface area, M^2/gm.
2.17	64.5	1.03
0.91	145	1.38
0.31	115	1.41

Discussion of k and N_0 Values

The k values were determined from the slopes of the ln $1/c$ versus time curves and the units are in (gm. moles/liter)$^{-1}$(min.)$^{-1}$. These k's are given for some of the conditions studied in Table X.

An increase in k was evident with an increase in flow rate at all the concentrations studied. The k values were independent of concentration in the ranges of column length and flow rate which did not approach critical values. At the

TABLE X

EFFECT OF INITIAL CONCENTRATION, FLOW RATE, AND COLUMN LENGTH ON k

Column length, cm.	k															
	c_0, 0.25%				c_0, 0.50%				c_0, 0.75%				c_0, 1.00%			
	313	625	967	1250	313	625	937	1250	313	625	937	1250	313	625	937	1250
	cm./min.															
2	205	383	642	1642	166	412	659	1053	241	382	441	836	251	309	545	1199
3	205	375	768	598	161	264	426	618	188	415	441	826	182	287	686	1191
4	–	205	402	536	161	238	426	547	–	155	441	800	182	252	668	982
5	205	375	402	473	166	184	426	516	188	176	453	–	182	252	668	601
6	–	232	–	473	–	–	426	390	140	–	–	794	–	–	343	498
7	–	375	–	–	–	211	426	390	–	179	–	794	–	204	390	482
8	–	–	–	–	–	–	–	–	–	–	–	–	–	193	287	–
Mean $k/L\times10^4$	667	619	664	595	798	475	496	468	605	492	481	648	636	440	546	660

concentration of 1.0% and flow rate 937 to 1250 cm. per min., there was an evident decrease in k with an increase in column length. A column length of 1 cm. always gave much higher k values than the succeeding column lengths.

Either the rate of diffusion to the surface or the speed of the surface reaction governs the rate of removal of the gas from the air stream, depending on which is the slower process. If k is dependent on flow rate, then diffusion is the rate-governing step. From Table X it is evident that k is proportional to L. Therefore, one can assume that mass transfer is the rate-controlling step and the surface reaction is much faster than the diffusion process.

In the present case in which the gas is removed by chemical reaction, N_0 should be directly correlated with the number of active oxygen atoms per cubic centimeter of reagent. Assuming that each molecule of silver permanganate has one atom of active oxygen for the oxidation of carbon monoxide to carbon dioxide and letting each active oxygen be represented by N_0, it was found by calculation from the amount of silver permanganate present per cubic centimeter of reagent in the reaction tube that $N_0 = 3.62 \times 10^{21}$. The calculation of N_0 from the slopes of column length versus breakdown time curves varied from 2.76×10^{21} to 4.1×10^{21} depending on the conditions. The mean value was 3.2×10^{21}. On comparing the two values of N_0 it may be assumed that nearly all of the molecules of silver permanganate are available for the reaction.

Conclusions

The relations between escaping concentration and time, column length and breakdown time, and flow rate and breakdown time, as predicted by the theory were found to hold for the solid–gas reaction of silver permanganate – zinc oxide and carbon monoxide. However, the predicted linear relation between the critical column length and the logarithm of the initial concentration was

not confirmed. Similarly, the reciprocal of the critical flow rate did not vary linearly with log c_0.

It was found that the critical column length increased with increasing flow rate but was unaffected by the initial concentration.

Diffusion, or mass transfer, of the gas molecules to the surface of the granules was determined to be the rate-controlling step as the rate constant varied directly with the flow rate. However, at initial concentrations and flow rates which approached critical values, the rate of transfer of heat was too slow to dissipate the heat of reaction. The granule bed, therefore, increased in temperature sufficiently to cause some thermal decomposition of the silver permanganate itself. This undoubtedly influenced the value of the rate constant at or near critical conditions. The rate constant, k, also depended inversely upon the mean granule diameter, in contrast to the results of other investigators on charcoal–gas systems, where k was found to be independent of granule size. With decreasing granule size, the breakdown time was found to increase at first, to pass through a maximum, and then to decrease.

The average value of N_0, the active centers, as obtained from experimental data, was 3.2×10^{21}. A calculated value, based on the assumption that each molecule of silver permanganate contains one atom of oxygen capable of oxidizing carbon monoxide, was in substantial agreement with the above, i.e., 3.62×10^{21}.

In view of the experimentally determined influences of granule size and other factors on the rate constant, the adsorption wave equation in its present form is not wholly applicable.

References

1. AMUNDSON, N. R. J. Phys. & Colloid Chem. 52: 1153. 1948.
2. BOHART, G. S. and ADAMS, E. Q. J. Am. Chem. Soc. 42: 523. 1920.
3. BRUNAUER, S., EMMETT, P. H., and TELLER, E. J. Am. Chem. Soc. 60: 309. 1938.
4. DANBY, C. J., DAVOUD, J. G., EVERETT, D. H., HINSHELWOOD, C. N., and LODGE, R. M. J. Chem. Soc. 918. 1946.
5. DUBININ, M. M. J. Russ. Phys. Chem. Soc. 62: 683. 1930.
6. GRANT, G. A., KATZ, MORRIS, and HAINES, R. L. To be published.
7. KATZ, MORRIS, and HALPERN, SOPHIE. Ind. Eng. Chem. 42 (No. 2): 345. 1950.
8. KATZ, MORRIS, and KATZMAN, J. Can. J. Research, F, 26: 318. 1948.
9. KLOTZ, I. M. Chem. Revs. 39: 241. 1946.
10. MECKLENBURG, W. Z. Electrochem. 31: 488. 1935.
11. WICKE, E. Kolloid Z. 93: 129. 1940.

CANADIAN JOURNAL OF RESEARCH

Notes on the Preparation of Copy

GENERAL:—Manuscripts should be typewritten, double spaced, and the **original and one extra copy** submitted. Style, arrangement, spelling, and abbreviations should conform to the usage of this Journal. Names of all simple compounds, rather than their formulae, should be used in the text. Greek letters or unusual signs should be written plainly or explained by marginal notes. Superscripts and subscripts must be legible and carefully placed. Manuscripts should be carefully checked before being submitted, to reduce the need for changes after the type has been set. If authors require changes to be made after the type is set, they will be charged for changes that are considered to be excessive. **All pages, whether text, figures, or tables, should be numbered.**

ABSTRACT:—**An abstract of not more than about 200 words, indicating the scope of the work and the principal findings, is required.**

ILLUSTRATIONS:

(i) *Line Drawings:*—All lines should be of sufficient thickness to reproduce well. Drawings should be carefully made with India ink on white drawing paper, blue tracing linen, or co-ordinate paper **ruled in blue only;** any co-ordinate lines that are to appear in the reproduction should be ruled in black ink. Paper ruled in **green, yellow, or red should not be used** unless it is desired to have all the co-ordinate lines show. Lettering and numerals should be neatly done in India ink preferably with a stencil (**do not use typewriting**) and be of such size that they will be legible and not less than one millimeter in height when reproduced in a cut three inches wide. All experimental points should be carefully drawn with instruments. Illustrations need not be more than two or three times the size of the desired reproduction, but the ratio of height to width should conform with that of the type page. **The original drawings and one set of small but clear photographic copies are to be submitted.**

(ii) *Photographs:*—Prints should be made on glossy paper, with strong contrasts; they should be trimmed to remove all extraneous material so that essential features only are shown. Photographs should be submitted **in duplicate;** if they are to be reproduced in groups, one set should be so arranged and mounted on cardboard with rubber cement; the duplicate set should be unmounted.

(iii) *General:*—**The author's name, title of paper, and figure number should be written in the lower left hand corner (outside the illustration proper) of the sheets on which the illustrations appear.** Captions should not be written on the illustrations, but typed on a separate page of the manuscript. All figures (including each figure of the plates) should be numbered consecutively from 1 up (arabic numerals). **Each figure should be referred to in the text.** If authors desire to alter a cut, they will be charged for the new cut.

TABLES:—Titles should be given for all tables, which should be numbered in Roman numerals. Column heads should be brief and textual matter in tables confined to a minimum. **Each table should be referred to in the text.**

REFERENCES:—**These should be listed alphabetically by authors' names, numbered in that order, and placed at the end of the paper.** The form of literature citation should be that used in the respective sections of this Journal. **Titles of papers should not be given in references listed in Sections A, B, E, and F, but must be given in references listed in Sections C and D.** The first page only of the references cited in papers appearing in Sections A, B, and E should be given. **All citations should be checked with the original articles.** Each citation should be referred to in the text by means of the key number; in Sections C and D the author's name and the date of publication may be included with the key number if desired.

Reprints

Fifty reprints of each paper without covers are supplied free. Additional reprints, if required, will be supplied according to a prescribed schedule of charges. On request, covers can be furnished at cost.